

Lawrence Berkeley National Laboratory

LBL Publications

Title

BONDING AND CHEMISTRY OF HYDROCARBON MONOLAYERS ON METAL SURFACES

Permalink

<https://escholarship.org/uc/item/1vj7b0nr>

Authors

Bent, B.E.

Somorjai, G.A.

Publication Date

1988-07-01

UC-401
LBL-25627

c.1

Center for Advanced Materials

CAM

RECEIVED
LAWRENCE
BERKELEY LABORATORY

JUN 7 1989

Presented at the Catalysts in Petroleum
Refining Conference, Kuwait, March 4-8, 1989,
and to be published in Applied Catalysis

LIBRARY AND
DOCUMENTS SECTION

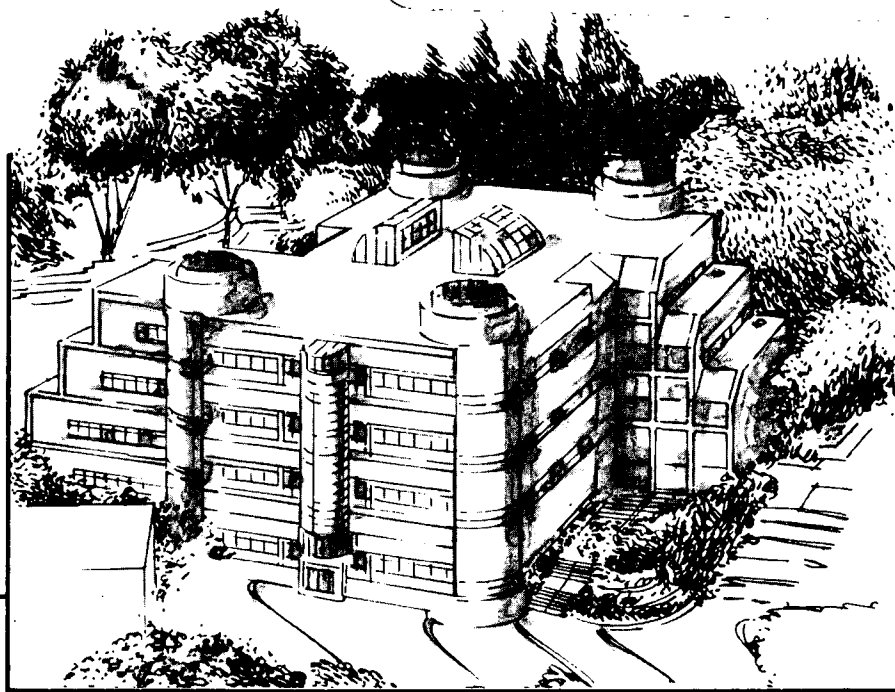
Bonding and Chemistry of Hydrocarbon Monolayers on Metal Surfaces

B.E. Bent and G.A. Somorjai

July 1988

For Reference

Not to be taken from this room



Materials and Chemical Sciences Division
Lawrence Berkeley Laboratory • University of California
ONE CYCLOTRON ROAD, BERKELEY, CA 94720 • (415) 486-4755

Prepared for the U.S. Department of Energy under Contract DE-AC03-76SF00098

LBL-25627
c.1

DISCLAIMER

This document was prepared as an account of work sponsored by the United States Government. While this document is believed to contain correct information, neither the United States Government nor any agency thereof, nor the Regents of the University of California, nor any of their employees, makes any warranty, express or implied, or assumes any legal responsibility for the accuracy, completeness, or usefulness of any information, apparatus, product, or process disclosed, or represents that its use would not infringe privately owned rights. Reference herein to any specific commercial product, process, or service by its trade name, trademark, manufacturer, or otherwise, does not necessarily constitute or imply its endorsement, recommendation, or favoring by the United States Government or any agency thereof, or the Regents of the University of California. The views and opinions of authors expressed herein do not necessarily state or reflect those of the United States Government or any agency thereof or the Regents of the University of California.

Bonding and Chemistry of Hydrocarbon Monolayers on Metal Surfaces

B.E. Bent^{} and G.A. Somorjai*

Department of Chemistry
and

Center for Advanced Materials, Lawrence Berkeley Laboratory
University of California, Berkeley, CA 94720

Abstract

Surface studies over the last ten years dramatically improved our understanding of how organic molecules react with metal surfaces.

Abstract

Results from ultra-high vacuum surface analysis techniques over the last ten years have dramatically increased our understanding of how unsaturated hydrocarbons react with metal surfaces. We review here what has been learned, utilizing results from our laboratory on the bonding and chemistry of ethylene and benzene to illustrate general principles. Several points deserve emphasis. First, clean surfaces of most transition metals (as might be expected from their coordinative unsaturation) are highly reactive towards unsaturated hydrocarbons, sequentially dehydrogenating these adsorbates over the temperature range of ~ 200 - 800 K to evolve hydrogen and deposit carbon. Throughout this temperature range, partially dehydrogenated decomposition intermediates can be isolated and identified. The bonding (and also possibly the chemistry) of these surface fragments is strikingly similar to that of hydrocarbon ligands in multinuclear organometallic clusters. Studies which combine reactions at atmospheric pressure with surface analysis in UHV show that these stable surface fragments are present on active hydrocarbon catalysts but are not reaction intermediates. It appears, however, that these surface organometallic compounds are important for promoting catalytic turnover of reactive species by tempering the surface reactivity through adsorbate-adsorbate interactions. Studies (under ultra-high vacuum conditions) of adsorbates at high surface coverages and in the presence of coadsorbates show dramatic effects of attractive and repulsive adsorbate-adsorbate interactions on the surface bonding and chemistry.

* Permanent Address: Department of Chemistry, Columbia University, New York, NY 10027

1. Introduction

During the last ten years modern surface science techniques have been applied to study the structure and bonding of small organic molecules adsorbed on metal surfaces. Ultra-high vacuum (UHV) systems such as that shown in Figure 1 have been extensively employed to study this chemistry on well-defined surfaces under controlled conditions. Typically, a single crystal having 1 cm^2 of surface area is used as the substrate. After mechanically polishing this substrate to a mirror finish, the sample is cleaned in ultra-high vacuum by a combination of chemical treatments (for example heating in oxygen to burn off carbon) and physical ion sputtering, followed by annealing to approximately two thirds the melting temperature to produce a well-ordered surface. Surface contamination at the level of 1% of a monolayer can be routinely detected by Auger electron spectroscopy or x-ray photoelectron spectroscopy and removed, while atomic periodicity over regions on the order of 100 \AA^2 or larger can be confirmed by diffraction of low energy electrons or helium atoms from the surface [1]. Once an ordered and clean single crystal surface such as those shown in Figure 2 is produced, it is exposed to a flux of hydrocarbon molecules at low pressures (10^{-9} - 10^{-8} Torr) to produce a partial or complete monolayer of adsorbed species. In this paper we review what has been learned about the bonding and chemistry of hydrocarbon monolayers on transition metal surfaces using results from our laboratory to illustrate general principles.

The two techniques most frequently used in our laboratory to study the structure and bonding of organic monolayers on metal surfaces are low-energy electron diffraction (LEED) [2] and high resolution electron energy loss spectroscopy (HREELS) [3]. The way these techniques are applied for determining the structure of adsorbed monolayers is shown schematically in Figures 2 and 3. For illustrative purposes, results from these techniques for ethylidyne (CCH_3) bonding to a Rh(111) surface are shown. Ethylidyne is the stable, room temperature species that forms spontaneously when ethylene is adsorbed on a Rh(111) surface

at room temperature. The identity of this species on Rh(111) and on the close-packed surfaces of several other group VIII metals has been substantiated by a variety of techniques, but the initial structural determination was made primarily by the combination of LEED and HREELS, techniques which we now briefly describe.

High resolution electron energy loss spectroscopy provides a vibrational spectrum of adsorbed molecules [3]. As shown in Figure 3A, when electrons are scattered from a surface, a small fraction (less than one percent) lose energy by exciting surface vibrations. With current technology, a low energy electron beam (1-200 eV) of sufficient intensity to detect the inelastically scattered electrons can be monochromatized to an energy spread of about 5 meV (40 cm^{-1}) full width half maximum. This resolution permits detection of energy losses due to vibrational excitation. The resulting energy loss vibrational spectrum for ethylidyne is shown in Figure 3B. This spectrum was assigned as shown in Figure 3D by comparison with the spectra of the ethylidyne ligand bound in trinuclear organometallic clusters. As we will emphasize in this paper, such a comparison is reasonable, since the bonding of organic fragments on metal surfaces closely parallels that of analogous ligands in organometallic chemistry [4].

In general, the surface vibrational spectrum provides several types of information about the bonding and identity of organic adsorbates. The surface vibrational frequencies can be used to determine functional groups and to detect bonding changes within functional groups upon adsorption on the surface. Deuterium labelling is extremely useful for discriminating CH and CC vibrations. The spectral intensities provide information about the adsorption site symmetry and bonding orientation through application of the selection rules for electron scattering and by consideration of how the oscillator strength of various vibrations will be effected by placing a vibrating dipole near a conducting substrate (Figure 3C) [3]. For the purposes of the studies discussed here, the surface dipole selection rule, which discriminates against vibrations of low symmetry or of orientation parallel

to the surface, was the only selection rule used to understand the nature of the bonding of adsorbed organic molecules.

While HREELS is particularly useful in identifying organic adsorbates, it does not provide a detailed adsorbate structure including bond lengths and bond angles. Low energy electron diffraction (LEED) nicely compliments HREELS in this respect. LEED utilizes the fact that the wavelength of 20-200 eV electrons is on the order of angstroms, a typical atomic separation in molecules. Elastic scattering of electrons in this energy range from adsorbate-covered surfaces therefore results in diffraction which can be analyzed to obtain adsorbate bond lengths and bond angles [2]. For example, if an adsorbate forms an ordered overlayer on a single crystal substrate, then the diffracted electrons will constructively interfere to produce a pattern of spots which can be imaged on a fluorescent screen in the LEED experiment. Such a pattern is shown in Figure 4 for an ordered (2x2) overlayer of ethylidyne species on a Rh(111) surface. [The notation (2x2) gives the dimensions of the overlayer unit cell relative to those of the substrate which are taken arbitrarily as (1x1).] The LEED spot intensities are a function of the structure of the adsorbed molecule. To determine this structure, the intensities of the diffracted electron beams are measured for various incident electron energies (wavelengths) to give what is called an I-V curve. Multiple scattering computations are then carried out on trial adsorbate geometries, frequently those suggested by information from HREELS, to obtain the best possible match with experiment. This procedure is similar in many respects to the analysis in x-ray diffraction, but is complicated by the multiple scattering of electrons which must be calculated [2].

While most of our studies have been carried out on single crystal surfaces, high-surface-area materials such as zeolites or metals dispersed on an oxide support can also be used in surface science studies to determine the structure of adsorbed organic molecules. Table 1 summarizes many of the techniques that are routinely applied to study the bonding of organic monolayers on both single cry-

stal and high-surface-area materials. Electron and ion scattering as well as molecular beam scattering techniques are eminently useful for studying the structure of external surfaces, while photon scattering techniques are a powerful probe for studies of the internal surfaces of porous materials. Organic adsorbates on dispersed materials have been successfully studied by magic angle spinning solid state NMR and by transmission infrared spectroscopy.

Most of our current understanding of how hydrocarbon monolayers bond to transition metal surfaces comes from studies of the group VIII metals. Among the pure metals, these are the most active catalysts for hydrocarbon transformations and are thus the most extensively studied. The hydrocarbon monolayers most frequently studied are those formed by adsorption of unsaturated alkenes and alkynes. These molecules bond strongly to clean, group VIII transition metal surfaces in contrast to saturated hydrocarbons which generally stick to transition metal surfaces only at either very low ($<150\text{K}$) or very high ($>800\text{K}$) temperatures. For example, normal alkanes adsorb on these surfaces at low temperatures by Van der Waals interactions, but they desorb molecularly at about their sublimation temperature (50-150K in UHV). At very high surface temperatures, n-alkanes will again stick to the surface because of their immediate decomposition to form surface carbon and gas phase hydrogen. Neither situation is conducive to studying the bonding of hydrocarbon monolayers. By contrast, alkenes and alkynes adsorbed on these surfaces below 200K generally decompose as the surface is heated through the formation of a series of hydrocarbon fragments which are stable in discrete temperature ranges [5]. These intermediates can be studied by LEED and HREELS.

We review here what has been learned about the bonding and chemistry of hydrocarbon monolayers on group VIII transition metal surfaces. To illustrate general principles we discuss results from our laboratory on the surface chemistry of ethylene and benzene on rhodium, platinum, and palladium surfaces. Our review focuses on three aspects of hydrocarbon surface chemistry: (1) the bonding

and reactivity of hydrocarbon monolayers on clean single crystal surfaces in ultra-high vacuum, (2) the effects of interactions between adsorbates on the surface bonding and chemistry, and (3) the relation between this chemistry in ultra-high vacuum and hydrocarbon catalysis at atmospheric pressures.

2. A Tale of Two Molecules: The Bonding and Chemistry of Ethylene and Benzene on Transition Metal Surfaces

2.1 Ethylene

A general feature of unsaturated hydrocarbon adsorption on clean transition metal surfaces (the coinage metals are a notable exception) is that it is largely irreversible. In other words, when one adsorbs an unsaturated hydrocarbon on a transition metal surface at low temperature and then heats the surface, the adsorbed molecule, rather than desorbing molecularly, will decompose to evolve hydrogen and leave the surface covered with carbon. Figure 5 shows the hydrogen evolution that is observed upon heating a Rh(111) surface covered at 100K with (A) ethylene, (B) propylene, (C) 1-butene, (D) cis-2-butene, and (E) isobutene. It is evident that these adsorbed alkenes sequentially dehydrogenate over a wide temperature range (about 500K) on Rh(111). Between the hydrogen desorption peaks there are temperature regimes where partially dehydrogenated intermediates are stable on the surface. It is of importance to determine the structure and bonding of these various surface fragments in order to understand why C-H bond breaking occurs over such a wide temperature range and to assess the role of these fragments in hydrocarbon catalysis which is typically carried out at about 500K, well above the temperature where hydrocarbon decomposition begins to occur.

Figure 6 shows the surface vibrational spectra obtained after adsorbing ethylene on a Rh(111) surface at 100K and heating to the indicated temperatures. The transformations with heating are irreversible in the sense that the resulting

monolayers can be cooled back down to 100K to record the HREEL spectra without changing the monolayer structure. As we will show later, these monolayers are also quite stable towards reversible hydrogenation in the presence of 1 atmosphere of hydrogen. The dramatic changes in the HREEL spectra of Figure 6 upon heating to 310 and 450K illustrate the sensitivity of surface vibrational spectroscopy for detecting the changes that occur in the adsorbed monolayer as ethylene becomes increasingly dehydrogenated.

The HREEL spectrum at 100K in Figure 6 has been attributed to ethylene adsorbed molecularly intact on the Rh(111) surface [6]. The vibrational frequencies, however, are markedly different from those for gas phase ethylene, indicating a strong interaction between ethylene and the rhodium surface. While the surface bonding geometry for this species has yet to be solved, a detailed analysis of the surface vibrational spectrum suggests that the molecule is bound with its carbon-carbon bond parallel to the surface analogous to the well-known Dewar-Chat-Duncanson mode of ethylene coordination in organometallic complexes. This type of coordination can give rise to the interactions shown in Figure 7. Depending on the metal surface involved, the degree of interaction between the bonding and antibonding π orbitals in ethylene and the empty and filled d orbitals in the metal can range from π to di- σ bonding as shown in Figures 7C and 7D. Based on the surface vibrational spectra reported for ethylene adsorbed molecularly on many transition metal surfaces, a wide range of interactions are indeed possible [6-8]. This is the first illustration of the similarity of the bonding of organic molecules on metal surfaces to the bonding of ligands in organometallic compounds.

When one increases the temperature of a Rh(111) surface covered with molecularly adsorbed ethylene to above 220K, ethylidyne (CCH_3) is formed, which has the vibrational spectrum shown in Figure 6B. To produce this surface fragment, one hydrogen atom is eliminated. Both LEED [9] and HREELS [10] confirm the bonding geometry for this species shown in Figure 8. Also tabulated in Figure 8 are the bond lengths and bond angles that have been determined for

ethylidyne adsorption on Pt(111) and for ethylidyne coordination in several trinuclear organometallic complexes [11]. The similarity between the cluster and surface bonding geometries is again noteworthy.

Ethylidyne is a common intermediate in the thermal chemistry of hydrocarbon monolayers on the Rh(111) surface. Besides its formation from ethylene, ethylidyne can also be generated at room temperature by dissociative adsorption of propylene, methylacetylene, or propadiene [12], and by coadsorption of acetylene and hydrogen [13]. While the surface bonding of ethylidyne has been most extensively studied on the Pt(111) and Rh(111) surfaces, this species has been isolated on the close-packed faces of several other metals, including Pd(111) [14] and Ru(001) [15]. Ethylidyne species have also been identified on the reconstructed Pt(100) surface which contains slightly buckled 3-fold sites [16]. It is presumed that on all these surfaces, ethylidyne bonds in the 3-fold site as it does on Pt(111) and Rh(111). Until recently, this bonding geometry was the only one identified for ethylidyne adsorption on surfaces. Other modes of alkylidyne coordination are, however, well-known in organometallic chemistry as shown in Figure 9 [17-20]. While the prevalence of 3-fold coordination on the transition metal surfaces implies that this bonding mode is favored over 1-fold and 2-fold coordination, the recent finding that ethylidyne species can be formed on a Rh(100) surface which lacks three-fold sites shows that other modes of ethylidyne coordination on surfaces are indeed possible [21].

Returning to the HREEL spectra of Figure 6, we see that ethylidyne decomposes on a Rh(111) surface when heated to 450K. As indicated, this spectrum has been attributed to a mixture of CH and C₂H species [12,22]. The general features of this spectrum remain unchanged throughout the temperature range of 450-800K, despite the continuous evolution of hydrogen from the surface (see Figure 5). Such behavior is consistent with a mixture of surface fragments, all of whom have similar vibrational spectra, but whose relative concentrations change throughout this dehydrogenation process. Our belief is that these species

are polymeric carbon chains terminated with hydrogen atoms and having the general formula C_xH . Increasing the surface temperature causes concurrent dehydrogenation and polymerization, eventually resulting in a graphitic monolayer. We show in Figures 10 and 11 that the first two members of this polymeric series, CH and C_2H , have analogues in organometallic chemistry. Similar species have been identified on Pd(111) [23], Ru(001) [15], Ni(110) [24], and, as indicated in Figure 11, Rh(100) [25].

It is educational to briefly compare the bonding and sequential dehydrogenation of C_3 hydrocarbons (propadiene, propylene, and methylacetylene) on Rh(111) [12] with the results discussed above for ethylene. As shown in Figure 12, a number of stable intermediates in the thermal decomposition of these molecules have been isolated and identified. With increasing temperature, the stable surface fragments are increasingly dehydrogenated. It is also evident that regardless of which parent hydrocarbon is adsorbed, if the temperature is high enough, then the same intermediates are formed. By contrast, at lower temperatures, the stable decomposition intermediates are strongly dependent on the nature of the parent hydrocarbon. In the case of ethylene, the both the molecular adsorption geometry and the decomposition intermediates are also highly dependent on the chemical nature of the metal and the structure of the surface. Many stable decomposition intermediates, including $CHCH_2$, $CHCH_3$, CCH_2 , CCH_3 , $CHCH$, CCH , and CH have been isolated on a variety of transition metal surfaces. The surface chemistry responsible for these intermediates will be commented on in Section 3.

2.2 Benzene

Like ethylene, benzene readily adsorbs on most clean transition metal surfaces and largely decomposes with heating as opposed to desorbing molecularly. Benzene decomposition, however, occurs at higher temperatures (generally above 350K as compared with 200-300K for ethylene). As a result, molecular benzene

adsorption can be readily studied at room temperature. Figure 13 compares HREEL vibrational spectra for saturation coverages of benzene adsorbed molecularly on Rh(100), Rh(111), and Pt(111) surfaces. The general features of all three vibrational spectra are quite similar, in contrast to molecular ethylene adsorption where the surface vibrational spectra vary dramatically both with the identity of the metal and with the surface geometry. The characteristic feature in the molecular benzene spectra is the intense mode at between 700 and 900 cm^{-1} . Isotope labelling studies show that this mode is due to a CH vibration, and by comparison with the vibrational spectrum for gas phase benzene, this mode has been assigned as the symmetric bending of all six hydrogen atoms out of the plane of the benzene ring (γ_{CH}). The strong intensity of this mode in the surface vibrational spectrum implies that the adsorbed benzene molecule bonds with its π ring parallel to the surface [26].

Such a bonding orientation is supported by LEED crystallography studies of adsorbed benzene on the Pd(111) [27], Rh(111) [28,29], and Pt(111) [30] surfaces. In order to perform these studies, it was necessary to coadsorb some carbon monoxide with the benzene in order to induce the benzene to form ordered structures on the surface. The packing of CO and benzene in two such ordered structures is shown in Figure 14. The interactions between benzene and carbon monoxide responsible for forming these molecular overlayers will be discussed below, but we note here that the surface vibrational spectra show no evidence for any kind of covalent bonding between the benzene and CO. Dynamical LEED analysis of these coadsorbed benzene/CO structures substantiates that benzene bonds with its π ring parallel to the surface on all three of these metals. The bonding within the benzene molecule, however, varies from one ordered structure to another, as shown in Table 2. In all cases, the benzene ring expands upon adsorption as indicated by the increase in the ring radii. While the degree of expansion is not always greater than the experimental uncertainty, the trend appears to be Pd(111) < Rh(111) < Pt(111). This trend, as shown in Table 2, can be nicely correlated with the shift in frequency of the γ_{CH} mode away from its gas phase

value in the surface vibrational spectrum. It is noteworthy that the frequency of this γ_{CH} mode has also been correlated both with the work function of the surface [26] and with the cohesive energy of the metal [31] on which the benzene is adsorbed.

Returning to the structural results in Table 2, it should be noted that the symmetry of the benzene ring expansion varies with the adsorption site, being 2-fold for the bridge site on Pt(111) and 3-fold in the case of the hollow sites on Rh(111) and Pd(111). In the latter cases, the adsorbed benzene has alternating long and short C-C bonds in the carbon ring, resulting in a Kekule-type structure. Once again, there is precedence for this type of bonding geometry from organometallic chemistry as shown in Figure 15 [32]. For the $c(2\sqrt{3}\times 4)\text{rect-C}_6\text{H}_6+\text{CO}$ structure on Rh(111), the C-C bond distances alternate between a very long 1.81Å and a short 1.33Å. This benzene appears almost as though it were three acetylene molecules; however, the expected Van der Waals separation between two acetylenes is on the order of 2.8Å, indicating that this adsorbate is still properly considered as a distorted benzene molecule. It should be noted that there is some controversy over the details of the benzene adsorption geometry. In particular, on the Rh(111) surface where the LEED [28,29] and HREELS [26,33] studies indicate a 3-fold symmetry for adsorbed benzene, ultra-violet photoelectron spectra have been used to infer a 6-fold symmetry [34]. On the other hand, recent studies utilizing scanning tunneling microscopy show evidence for a 3-fold distortion in the benzene ring of the (3x3) structure on Rh(111) [35].

It is intriguing to consider how the observed distortion in the adsorbed benzene molecule may correlate with its subsequent decomposition pathway. In the case of benzene decomposition on Rh(111) the decomposition fragments determined by HREELS are compared in Figure 16 with those discussed above for ethylene. The significant result for this discussion is that first stable decomposition intermediates for benzene have been identified as CH and C_2H . These fragments are also the stable decomposition intermediates for acetylene at this tem-

perature. It has been hypothesized [36] that, consistent with the 3-fold distortion determined by LEED, benzene decomposes via 3 acetylenes, which are unstable at the decomposition temperature and immediately dehydrogenate to CH and C₂H. In this regard, it is interesting that Pd(111), which induces the least distortion in adsorbed benzene (Table 2), is an active surface for the trimerization of acetylene to benzene [37].

3. Organometallic Analogues for Hydrocarbon Monolayer Chemistry

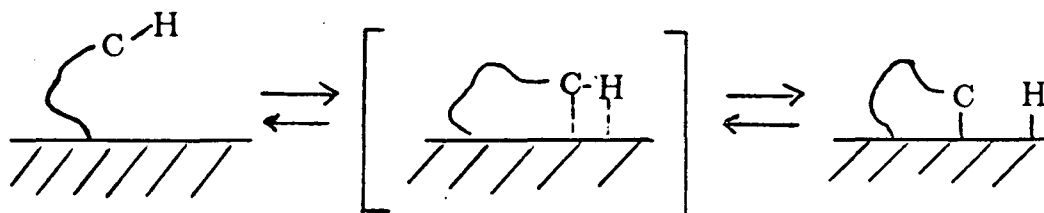
Sequential dehydrogenation over a wide range of temperature, as illustrated above for benzene and ethylene adsorption, is typical for hydrocarbon adsorption on clean transition metal surfaces. The particular intermediates which are stable vary both with the chemical identity of the metal and with the structure of the surface. The wide range of structures observed makes generalizations about the chemistry difficult, but it is clear that in the stoichiometric reactions between unsaturated hydrocarbons and transition metal surfaces, C-H bonds are readily broken. Ethylene generally begins to dehydrogenate at measureable rates between 200 and 300K. These temperatures, assuming typical unimolecular decomposition preexponential factors of 10^{13} s^{-1} , correspond to activation energies of 8-15 kcal/mol. Since this value is much less than gas phase C-H bond dissociation energies of >90 kcal/mol, this metal-assisted C-H bond breaking is called C-H activation [38].

The degree to which C-H bonds are activated depends on metal atomic number, surface roughness, and the identity of the adsorbed hydrocarbon fragment. It appears, in general, that early transition metals, rough surfaces, and surface fragments having the fewest metal-carbon bonds show the most C-H activation. These observations can be rationalized using elementary kinetic and thermodynamic arguments along with well-known reaction pathways in organometallic chemistry. While these explanations, as discussed below, are based largely on analogy to the solution chemistry of hydrocarbon ligands in organome-

tallic compounds and are not theoretically rigorous [39] or experimentally proven, such considerations are, we feel, useful in providing a conceptual framework in which the numerous experimental results for hydrocarbon adsorption on metal surfaces can be summarized. Further, the striking structural analogies between hydrocarbon adsorbates on metal surfaces and hydrocarbon ligands in organometallic clusters discussed above are suggestive of reactive parallels between these systems.

It should be noted first that low activation energies for C-H bond breaking on metal surfaces are possible because metal-carbon, metal-hydrogen, and possibly carbon-carbon bonds form simultaneously with C-H bond breaking. Thermodynamics requires that at least two of these types of bonds be formed, since $E(\text{M-H}) \simeq 60 \text{ kcal/mol}$ [40], $E(\text{M-C}) \simeq 30\text{-}60 \text{ kcal/mol}$ [41], and $E(\text{C-C}) \simeq 60 \text{ kcal/mol}$ (the difference between C-C single and double bond energies). If only one of these bonds forms upon C-H bond breaking, the minimum activation energy for C-H bond breaking would be at least 30 kcal/mol (the endothermicity of the reaction). Since the experimental activation energies are less, such free radical chemistry can be ruled out as the mechanism for C-H bond breaking.

The simplest mechanism for elementary dehydrogenation that is probably energetically downhill and is also well-established in organometallic chemistry is:



The overall process is called an oxidative addition in organometallic chemistry, since the metal atom(s) formally donate(s) two electrons to form the metal-carbon and metal-hydrogen bonds [42]. The reverse process which results in C-H bond formation is called a reductive elimination. In surface chemistry, these reactions are generally called hydrogenations and dehydrogenations. The oxidative

addition/reductive elimination formalism and the analogy between surface and organometallic chemistry were first extensively applied to rationalize surface chemical reactions by E.L. Muetterties [41,43,44].

The term oxidative addition does not imply any mechanism or transition state as shown in brackets above. It appears likely, however, that while "the geometric features of the oxidative addition reaction may comprise an initially linear M-H-C interaction, ultimate C-H bond cleavage requires a triangular M-H-C interaction. [41]" Such 3-center interactions are observed in a number of stable organometallic complexes [41]. An implication of this C-H bond breaking mechanism is that the rate of bond breaking will depend strongly on the proximity of the C-H bond to the metal atom or metal surface. Muetterties has noted examples of hydrocarbon surface chemistry supporting this proximal effect [41], and several other experimental results deserve mention here.

As noted previously, there is generally $\sim 600\text{K}$ between the temperature at which C-H bonds begin to break and complete dehydrogenation. Differences in C-H bond energies cannot begin to account for this enormous variation in the C-H bond breaking rate. The proximal effect, on the other hand, can account for the large variations in both the activation energy and the preexponential factors that are observed. For example, based on this geometric model, it is not surprising that ethylidyne, whose C-H bonds are far removed from the surface, has an activation energy for decomposition of 27 kcal/mol compared to 17 kcal/mol for conversion of ethylene to ethylidyne where the molecular adsorption of ethylene places the C-H bonds in close proximity to the surface. Likewise, preexponential factors for some "unimolecular" dehydrogenations suggest a geometrically demanding transition state which might be expected for a triangular M-H-C interaction [45]. The experimentally-determined values of 10^9 for ethylidyne decomposition on Pt(111) [46] and for methanol decomposition on Ni(100) [47] are 10^4 lower than expected for unimolecular decomposition, suggesting a large entropy of activation.

While dehydrogenation has been stressed so far, there is also experimental evidence for the reverse hydrogenation (reductive elimination) reaction in the chemistry of hydrocarbon monolayers on metals. Such a reaction is implicated, for example, by the formation of methane in ethanol decomposition on Ni(111) [48], methane formation in acetaldehyde decomposition on a stepped platinum surface [49], ethylene hydrogenation to ethane on Pt(111)

[50], and ethylidyne H,D exchange on Rh(111) [10]. While it is possible that some of the products mentioned above are formed by a mechanism other than hydrogenation (for example, an intramolecular hydrogen shift), we favor elementary hydrogenation/dehydrogenation steps to explain the observed surface chemistry based on the prevalence of these reactions in organometallic chemistry.

Thus, we view the chemistry of hydrocarbon monolayers on metals as a combination of elementary hydrogenation (reductive elimination) and dehydrogenation (oxidative addition) steps. For example, the surface fragments and gas phase products formed by ethylene adsorption on transition metals can be rationalized by the reaction steps shown in Figure 17. Under ultra-high vacuum conditions (with a negligible partial pressure of hydrogen), the experimental data suggest that dehydrogenation is generally favored. However, the potential importance of surface hydrogen atoms should not be overlooked. In particular, since barriers to surface diffusion are generally 20-30% of those for desorption, once hydrogen atoms are formed during dehydrogenation, they can diffuse thousands of angstroms across the surface before desorbing. If the rate of hydrogenation of any of the surface fragments is faster than the rate of hydrogen desorption, then the fragment should be readily hydrogenated.

We have recently utilized this idea along with experimental observations and molecular orbital calculations in the literature to propose a new mechanism for ethylidyne formation [51]. In this mechanism, ethylene conversion to ethylidyne is initiated by hydrogenation to form C_2H_5 followed by sequential dehydrogenation at the α -carbon to give CCH_3 . The mechanism and its associated

energetics derived based on a combination of theory [39a] and experiment [50] are shown in Figure 18A and are compared with those for a previously proposed mechanism for ethylidyne formation Figure 18B. It should be noted that one hydrogen atom is needed to initiate our proposed mechanism of ethylidyne formation. However, once the first C_2H_5 species is generated (possibly by residual hydrogen atoms which will always be present), two hydrogen atoms are produced in the formation of ethylidyne and can initiate further conversions of ethylene to ethylidyne. Significant experimental observations with regard to the intermediacy of C_2H_5 in this mechanism are that (1) ethylene can be hydrogenated to ethane on Pt(111) at temperatures below where ethylidyne forms [50], (2) ethylidyne adsorption on Pt(111) at room temperature generates ethylidyne [22], and (3) the metals which convert ethylene to ethylidyne are among the most active catalysts for ethylene hydrogenation.

4. Coadsorption of Molecules. Attractive and Repulsive Adsorbate-Adsorbate Interactions

An important feature of the chemistry of adsorbed monolayers in general is the significance of interactions between adsorbates. While it is difficult to quantitatively determine the magnitude and spatial extent of these interactions, the resulting effects on both the surface bonding and chemistry can be dramatic. A most studied example of repulsive adsorbate-adsorbate interactions has been the effect of high surface coverages on the heat of adsorption of carbon monoxide. The effect is illustrated in Figure 19 for carbon monoxide adsorption on a Pd(111) surface. At low coverages, the heat of adsorption is roughly constant, since the molecules are far apart from each other and the heat of adsorption is dominated by the adsorbate-substrate interaction. At about half a monolayer, an ordered structure forms and there is a drastic decrease in the heat of adsorption. Infrared spectroscopy studies suggest that the decreased heat of adsorption in this ordered structure is due both to dipole-dipole interactions between adjacent CO's and a shift in the adsorption site on the surface from 3-fold hollow to 2-fold bridge [52].

The further decrease in the heat of adsorption at higher coverages may also be due to a combination of subtle changes in the bonding site and increased repulsive interactions between adsorbates. There is evidence for such high coverage effects from LEED studies of carbon monoxide adsorption on a Rh(111) surface. It is found, as shown in Figure 20, that for the highest attainable coverages of CO, the molecules pack onto the surface to be far apart from one another. In order to achieve this pseudohexagonal overlayer, however, the adsorbates can no longer all bond in the high symmetry sites on the surface, with some CO molecules being displaced slightly from bonding directly on top of a Rh atom [53]. This structure apparently represents a balance between repulsive adsorbate-adsorbate interaction and attractive adsorbate-substrate ones.

An extreme case of attractive interactions between adsorbate molecules occurs when one adsorbate, such as an alkali metal atom, induces dissociation of another adsorbate such as carbon monoxide. This dissociation reaction can be monitored by coadsorbing isotopically-labelled $^{13}\text{C}^{16}\text{O}$ and $^{12}\text{C}^{18}\text{O}$ with the alkali metal followed by thermally desorbing the carbon monoxide. If dissociation occurs on the surface, desorption of the cross product $^{13}\text{C}^{18}\text{O}$ is observed. Figure 21 plots the amount of carbon monoxide that is dissociated on a Rh(111) surface precovered with potassium in such an experiment [54]. At 20% of a monolayer of potassium coverage, up to 3 carbon monoxide molecules are dissociated per potassium atom, while in the absence of potassium, no carbon monoxide is dissociated on the Rh(111) surface at low pressures.

Coadsorbate interactions in hydrocarbon monolayers are less-studied than those discussed above for carbon monoxide, but there is evidence for both attractive and repulsive interactions which affect the bonding and chemistry. Repulsive interactions are implicated in the molecular desorption of ethylene observed at high surface coverages on many transition metals. For example, at low ethylene coverages on Rh(111), all of the adsorbed ethylene fragments by the pathways described above, while ethylene adsorbed in excess of $\Theta = 0.25$ (number of

ethylene per surface Rh atom) desorbs molecularly [6]. Attractive interactions are evident in the coadsorption of carbon monoxide with a number of organic adsorbates. Figure 22 shows the effect that carbon monoxide has on the long range order of ethylidyne species on a Rh(111) surface. In the absence of carbon monoxide, an ethylidyne monolayer shows no long range order on this surface at room temperature, but when coadsorbed with CO, the adsorbates form an intermixed, ordered $c(4 \times 2)$ structure as shown. Similarly, benzene does not generally form ordered monolayers on transition metal surfaces, but many ordered structures have been observed on Pt(111), Pd(111) and Rh(111) when benzene is coadsorbed with carbon monoxide. This ordering of CO with hydrocarbon adsorbates can be correlated with the changes in work function observed upon adsorption [55]. In particular, a classical interpretation of the work function changes in terms of induced dipoles at the surface leads to the conclusion that CO and the organic adsorbates will form dipoles which are antiparallel, leading to an attractive interaction between these two adsorbates. Further, it is significant that adsorbates which are predicted to have parallel dipole moments do not form intermixed, ordered structures when coadsorbed.

Carbon monoxide coadsorption can also alter the thermal decomposition pathways of hydrocarbon adsorbates [56]. The effect of carbon monoxide on the chemistry of ethylene on Rh(111) and Rh(100) surfaces is summarized in Figure 23. While ethylene chemistry on Rh(111) appears to be relatively insensitive to the presence of coadsorbed CO, the chemistry on Rh(100) depends on the coverage of both CO and ethylene [57]. In the absence of CO and for low exposures of ethylene, the primary decomposition product is C_2H . At higher exposures, CCH_3 species are also formed. By preadsorption of a half a monolayer of CO, the production of C_2H can be completely suppressed, and subsequent ethylene adsorption yields only CCH_3 . These interesting effects which occur as a result of high coverages of adsorbates or the coadsorption of molecules are of importance for understanding catalytic surface reactions which are carried out with high pressures and mixtures of gases.

5. Organic Monolayers and Catalysis

The question arises as to what role these stable surface fragments which are formed in ultra-high vacuum and which have structures analogous to hydrocarbon ligands in organometallic clusters play in catalytic hydrocarbon conversion reactions over transition metal surfaces. In order to investigate this question we have studied various catalytic reactions in a high-pressure/low-pressure apparatus such as that shown in Figure 1. Besides the surface analysis techniques in this apparatus which were commented upon previously, this system has the capability (as shown in Fig. 1b) to enclose the well-characterized single crystal wafer inside a tube which can be pressurized to an atmosphere or more with reactant gases while still maintaining ultra-high vacuum in the surrounding chamber [58]. The single crystal can then be heated to induce a catalytic reaction whose products are sampled and quantified by gas chromatography. Periodically, the reaction is interrupted, the high-pressure cell evacuated, and the crystal returned to UHV for surface analysis. In this way, the effects of hydrocarbon monolayer structure on the catalytic reaction rate and vice versa can be studied. We illustrate the significant findings obtainable from this experimental approach using our studies of ethylene hydrogenation and of hydrocarbon conversion reactions.

5.1 Ethylene Hydrogenation

This stoichiometrically simple reaction combines ethylene and hydrogen to give ethane. Despite extensive studies over the last 50 years, the surface reaction mechanism in this heterogeneously catalyzed process remains controversial. It is generally accepted, however, that while the form of the metal catalyst (foils, wires, powders, films) has little effect on hydrogenation activity, catalyst preparation can have dramatic effects [59]. Utilizing single crystal surfaces as model catalysts we have investigated the nature and function of adsorbed monolayers on this reaction.

We found that catalytic ethylene hydrogenation is facile over both Pt(111)

and Rh(111) surfaces at room temperature. The hydrogenation rates and kinetic parameters are comparable with those reported for foils, wires, or dispersed metal particle catalysts [22,60], suggesting that these single crystal surfaces are reasonable model systems. Auger electron spectra of Pt(111) and Rh(111) surfaces after pumping out the hydrogenation reaction mixture and returning the single crystal catalysts to ultra-high vacuum show that the surfaces of both metals are covered with about a half monolayer of carbon (one carbon per two metal atoms). Nearly 100% of this carbon is partially hydrogenated and, as shown in Figure 24 for a Rh(111) surface, exists on the surface as ethylidyne species. Analogous results for a Pt(111) catalyst have been published [61]. It was found that these monolayers of ethylidyne were quite stable under one atmosphere of hydrogen or deuterium [6,63]. As shown in Figure 25, both the rate of rehydrogenation and removal of ethylidyne from the surface and the rate of H,D exchange in the ethylidyne methyl group are orders of magnitude slower than the rate of catalytic ethylene hydrogenation. On the other hand, it was also found that these monolayers of ethylidyne, despite their stability in high pressures of hydrogen, do not poison the catalytic hydrogenation reaction. Thus, any structural changes which occur in the adsorbed monolayer during transfer of the working catalyst to UHV must be reversible. To confirm the stability of ethylidyne under reaction conditions, ethylene hydrogenation was carried out over a Rh(111) surface precovered with a monolayer of CCD_3 . After running the hydrogenation to a turnover number of 500 (number of ethane molecules produced per surface Rh atom) at 300K, the ethylidyne monolayer still contained a substantial fraction of its original deuterium atoms. These experiments show that the strongly-bound carbonaceous species (ethylidyne under UHV conditions) on these active catalysts is not a hydrogenation intermediate but is instead a part of the catalyst. Infrared studies of supported Pd catalysts *during* catalytic ethylene hydrogenation support this conclusion [63].

How, then, do these ethylidyne-covered surfaces catalyze the hydrogenation of gas phase ethylene? Two possible mechanisms which have been proposed

are shown in Figure 26. Both mechanisms utilize the observation that ethylidyne-covered surfaces are found to be capable of dissociating hydrogen under high pressures of hydrogen [50]. In the upper mechanism, this surface hydrogen is then transferred up to gas phase ethylene via formation of ethylidene (CHCH_2) species on the surface. This mechanism presumes that ethylene hydrogenation occurs over the majority of the surface and seeks to explain how ethylene can be catalytically hydrogenated when the ethylidyne monolayer prohibits adsorption of this molecule directly onto the metal surface where the dissociated hydrogen is bound. Objections to this mechanism stem from what appears to be an entropically and enthalpically unfavorable transition state, and from the fact that the observed H,D exchange in the reactant ethylene is not accounted for. The lower mechanism in Figure-26 overcomes these objections by presuming that ethylene can somehow reach the metal surface despite the presence of an ethylidyne monolayer. This adsorption could occur at imperfections in the ethylidyne monolayer or in between ethylidyne species if there is enough diffusion and compression of the layer under high pressure conditions. Once the ethylene reaches the surface, it can be hydrogenated sequentially, as shown, by a Horiuti-Polanyi [59] mechanism. Reversibility in the the first hydrogenation step accounts for H,D-exchange in ethylene. While ethylidyne plays no direct role in this latter mechanism, it may act as a kind of "shade tree" on the surface, prohibiting adsorption of any large catalyst poisons while still permitting hydrogen adsorption and dissociation. Further studies utilizing high Miller-index single crystals (having steps and kinks) and isotope labelling to study the hydrogenation both of ethylene and other alkenes and alkynes are needed to determine the mechanistic details of catalytic hydrogenation.

5.2 Hydrocarbon Conversion Reactions

While the rate of catalytic ethylene hydrogenation appears to be relatively insensitive to the geometry of the catalyst surface, most hydrocarbon reactions catalyzed by transition metal surfaces are strongly affected by the surface atomic

arrangement. Hydrocarbon conversion reactions are some of these. The term hydrocarbon conversion refers to those reactions associated with converting the mixture of hydrocarbons found in petroleum into high octane gasoline. The best catalyst among the pure metals for these reactions is platinum. As shown in Figure 27, a suitably prepared platinum catalyst heated to between 500 and 750K is able to convert a straight chain hydrocarbon such as n-hexane into isomers, rings, aromatics, and shorter chain hydrocarbons. The reactions leading to branched isomers (isomerization) and cyclic molecules (dehydrocyclization) are especially desirable for producing high octane gasoline from petroleum naphtha. The hydrogenolysis reactions which produce lower molecular weight, gaseous products are undesirable. The selectivity (yield of a given product/ total yield) of a platinum catalyst for producing these various products varies with temperature. Since both dehydrocyclization and isomerization have relatively high activation energies (in the range of 25-40 kcal/mol), they proceed at a higher rate relative to hydrogenolysis as the temperature increases. This consideration is counterbalanced by the higher rate of deactivation or "cokeing" that occurs with increasing temperature, due to the formation of an unreactive carbon deposit on the catalyst surface.

Answers to how the geometry of platinum surface effects the selectivity of hydrocarbon conversion reactions have been obtained by studying platinum single crystal surfaces in a high-pressure/low-pressure apparatus such as that discussed above [64]. A variety of high-Miller-index surfaces containing ordered and quantified concentrations of steps and kinks (see Figure 2) were utilized in these studies. By measuring the rates of various model hydrocarbon conversion reactions over these geometrically well-defined surfaces, it was found that dehydrocyclization is substantially more facile on the hexagonal Pt(111) surface than on the square Pt(100) surface [65]. This result is shown for n-hexane and n-heptane aromatization in Figure 28. By contrast, isomerization of isobutane (Figure 29) is significantly faster over a Pt(100) surface than over Pt(111), and hydrogenolysis rates, as shown in Figure 29, are maximized on the Pt(10,8,7) surface which contains a high concentration of kink sites [66]. It is, therefore, evident that the rela-

tive rates (the selectivity) of these hydrocarbon conversion reactions are indeed a strong function of the platinum surface geometry.

As for ethylene hydrogenation above, the detailed surface reaction mechanisms for hydrocarbon conversion reactions over these single crystal platinum surfaces are not yet evident. We do know, however, that the working catalyst surface is not pure platinum, but rather a surface covered with a high coverage of strongly bound carbonaceous fragments. The residence time of this carbonaceous deposit under catalytic reaction conditions was determined by ^{14}C labelling studies [62]. Carbon-14 is a β particle emitter, so its surface concentration as a function of time during the catalytic reaction could be monitored using a semiconductor detector. The hydrogen content of the adsorbed organic layer was determined by thermally decomposing the adsorbed layer and detecting the amount of desorbing hydrogen with a mass spectrometer. From these investigations, it was found that the residence time of the adsorbed carbonaceous layer depends on its hydrogen content, which in turn depends on the reaction temperature as shown in Figure 30. While the amount of the deposit does not change with temperature, its composition does, becoming poorer in hydrogen as the reaction temperature increases [67]. The important observation as far as the role of this carbonaceous deposit in catalysis is concerned is that at any given temperature, the residence time of the surface fragments are substantially larger than the turnover frequency of the catalytic reactions carried out at that temperature. We are therefore lead to conclude, as we did previously for ethylene hydrogenation, that these strongly bound hydrocarbon fragments, while present on active catalysts, are not catalytic intermediates under most conditions.

While not participating directly in the catalytic reactions, this hydrocarbon monolayer does, no doubt, serve a useful role on the catalyst surface by tempering the surface reactivity. It is clear from studies both in ultra-high vacuum (negligible partial pressures of hydrogen) and under catalytic reaction conditions (hydrogen pressures above 1 atm), that dehydrogenation is the strongly favored over hy-

drogenation or molecular desorption on *clean* platinum (and many other transition metal) surfaces. On the other hand, it is also clear from studies in ultra-high vacuum that high coverages of these strongly-bound, organometallic surface fragments inhibit dehydrogenation and enhance molecular desorption of coadsorbed molecules. For example, as noted above, *clean* Rh(100) surfaces dehydrogenate ethylene at room temperature to C_2H ; however, once the coverage exceeds half a monolayer, the more hydrogen-rich CCH_3 species begin to form. Clean Rh(111) surfaces dehydrogenate ethylene (up to a quarter of a monolayer) to CCH_3 , but ethylene in excess of this coverage desorbs molecularly.

The discussion above illustrates a maxim often cited in enzymatic catalysis that the most active catalysts represent a compromise between transition state stabilization and tight binding of the reactants and products [68]. Clean platinum surfaces bind unsaturated hydrocarbons too strongly to catalytically "turn-over" these molecules at measureable rates. Graphite covered surfaces, however, do little to stabilize the reaction transition state. Surfaces covered with monolayer quantities of partially hydrogenated adsorbates apparently represent a reasonable compromise that permits the intermediate bonding strength to the surface required for catalytic turnover. The molecular details of the interactions between catalytic reactant(s) and the sterically crowded active surface site are important questions for future research to address. Isotope labelling studies certainly will play an important role in this endeavor. We also believe that understanding the general principles of C-H and C-C bond chemistry on transition metal surfaces through studies of hydrocarbon adsorption on single crystal surfaces in ultra-high vacuum will prove useful for designing new generations of selective catalysts. While such principles are not yet well-established, a substantial data base of experimental results is rapidly accumulating and in Section 3 of this paper we have utilized reactions from organometallic chemistry to rationalize some of the general observations.

6. Future Studies

The surface science techniques that have become available during the past two decades are eminently useful in studies of the structure and bonding of organic molecules adsorbed on metal surfaces. The two examples given here, ethylene and benzene, illustrate the general features of hydrocarbon monolayer chemistry on transition metal surfaces. The temperature-dependent, sequential decomposition observed, and the similarity of the resulting strongly adsorbed surface species to hydrocarbon ligands in multinuclear organometallic complexes all indicate the richness and diversity of two-dimensional organometallic chemistry. The available experimental results also indicate that the strongly adsorbed organometallic species on the surface play only a secondary or peripheral role in catalytic hydrocarbon surface reactions. Catalysis must occur at active sites embedded in these two-dimensional organometallic layers.

In the future, it is imperative that we study the organic surface chemistry of a wider range of molecules. Chemical variations on simple hydrocarbons (for example the addition of heteroatoms such as nitrogen, sulfur, or oxygen) can provide many insights. Only after the accumulation of a great deal of data will the systematic patterns of surface bonding and reactivity emerge. Another direction that studies of organic monolayers will take is the investigation of their adsorption on surfaces having a large concentration of defects (steps and kinks). Two such surfaces are shown in Figure 2. Up to now, most of the studies of organic monolayers have focused on flat, rather structurally uniform surfaces. It is evident that the presence of defects can have great catalytic significance, indicating that bond breaking activity is very different at these differently coordinated surface sites. In addition to the relevance of such studies for heterogeneous catalysis, the surface chemistry of hydrocarbon ligands is relevant for the deposition of thin films by metal-organic chemical vapor deposition (MOCVD) [69].

Another major area of organic surface chemistry for the future is the study of organic molecules at solid-liquid and solid-solid interfaces. Electrochemical studies in solution coupled with spectroscopic studies in ultra-high vacuum have

demonstrated the substantial effects of solution pH and electrode potential on the bonding of hydrocarbon monolayers [70]. The scanning tunneling microscope that has been recently developed also appears to be an excellent technique for a molecular level study (potentially in conjunction with electrochemistry) of adsorbed organic monolayers at solid-liquid interfaces [71]. A third technique that is opening up investigations at solid-liquid interfaces is second harmonic generation [72]. This technique monitors photons of frequency 2ω when an incident laser beam at frequency ω is reflected from a surface. The generation of this second harmonic light is a property of surfaces which can be exploited to study both solid-liquid and solid-solid interfaces. A modification of this technique is sum frequency generation when two lasers operating of frequencies w_1 and w_2 generate light at the sum frequency, $w_1 + w_2$. If one of the lasers is tuneable, the variable sum frequency permits taking vibrational spectra of molecules adsorbed at the solid-liquid or solid-solid interface. Studies utilizing second harmonic and sum frequency generation could also be carried out in a diamond anvil cell to potentially study organic monolayers between two solid surfaces under high pressures. Such monolayers at high pressures are of practical importance for understanding the bonding and chemistry of lubricants under conditions of friction and wear. These are just some of the many frontiers in organic surface chemistry that emerge from recent surface science studies. It is hoped that researchers in the field of surface science and organic chemistry will pursue investigations in these important areas.

Acknowledgements

This work was supported by the Director, Office of Energy Research, Office of Basic Energy Sciences, Materials Sciences Division, U.S. Department of Energy under Contract Number DE-AC03-76SF00098.

References

1. For an introduction to preparation and analysis of single crystal surfaces in ultra-high vacuum, see Ertl, G; Kupperts, J. *Low Energy Electrons and Surface Chemistry, second edition*; VCH Publishers: Deerfield Beach, FL, 1985.
2. Clarke, L.J. *Surface Crystallography: An Introduction to Low Energy Electron Diffraction*; John Wiley: New York, 1985.
3. Ibach, H.; Mills, D.L. *Electron Energy Loss Spectroscopy and Surface Vibrations*; Academic: New York, 1982.
4. An excellent monograph on the surface/cluster analogy is: Albert, M.R.; Yates, Jr., J.T. *The Surface Scientist's Guide to Organometallic Chemistry*; American Chemical Society, Washington D.C., 1987.
5. Somorjai, G.A.; Bent, B.E. *Progress in Colloid and Polymer Science* **1985**, *70*, 38.
6. Bent, B.E.; Mate, C.M.; Kao, C-T.; Slavin, A.J.; Somorjai, G.A. *J. Phys. Chem.* in press.
7. Sheppard, N. *J. Electron Spectrosc. Related Phenom.* **1986**, *38*, 175.
8. Stuve, E.M.; Madix, R.J. *J. Phys. Chem.* **1985**, *89*, 3183.
9. Koestner, R.J.; Van Hove, M.A.; Somorjai, G.A. *Surf. Sci.* **1982**, *121*, 321.
10. Koel, B.E.; Bent, B.E.; Somorjai, G.A. *Surf. Sci.* **1984**, *146*, 211.
11. Koestner, R.J.; Van Hove, M.A.; Somorjai, G.A. *J. Phys. Chem.* **1983**, *87*, 203.
12. Bent, B.E.; Mate, C.M.; Crowell, J.E.; Koel, B.E.; Somorjai, G.A. *J. Phys. Chem.* **1987**, *91*, 1493.

13. Dubois, L.H.; Castner, D.G.; Somorjai, G.A. *J. Chem. Phys.* **1980**, *72*, 5234.
14. Gates, J.A.; Kesmodel, L.L. *Surf. Sci. Lett.* **1982**, *120*, 1461.
15. Hills, M.M.; Parmeter, J.E.; Mullins, C.B.; Weinberg, W.H. *J. Am. Chem. Soc.* **1986**, *108*, 3554.
16. (a) Ibach, H. *Proc. Int. Conf. Vibrations Adsorbed Layers, Julich* **1978**, 64.
(b) Hatzikos, G.H.; Masel, R.I. *Surf. Sci.* **1987**, *185*, 479.
17. 1-fold coordination: Fischer, E.O.; Schubert, U.; Fischer, H. *Pure and Appl. Chem.* **1978**, *50*, 857.
18. 2-fold coordination: (a) Ashworth, T.V.; Howard, J.A.K.; Stone, F.G.A. *J. Chem. Soc., Dalton Trans.* **1980**, 1609. (b) Davis, D.L.; Dyke, A.F.; Endesfelder, A.; Knox, S.A.R.; Naish, P.J.; Orpen, A.G.; Plaas, D.; Taylor, G.E. *J. Organomet. Chem.* **1980**, *198*, C43. (c) Evans, J.; McNulty, G.S. *J. Chem. Soc., Dalton Trans.* **1984**, 79.
19. 3-fold coordination: Skinner, P.; Howard, M.W.; Oxtan, I.A.; Kettle, S.F.A.; Powell, D.B.; Sheppard, N. *J. Chem. Soc., Faraday Trans. 2* **1981**, *77*, 1203.
20. 4-fold coordination: Eady, C.R.; Fernandez, J.M.; Johnson, B.F.G.; Lewis, J.; Raithby, P.R.; Sheldrick, G.M. *J. Chem. Soc., Chem. Comm.* **1978**, 421.
21. Slavin, A.J.; Bent, B.E.; Kao, C-T.; Somorjai, G.A. *Surf. Sci.* in press.
22. Bent, B.E. Ph.D. Dissertation, University of California, Berkeley, 1986.
23. Kesmodel, L.L.; Waddill, G.D.; Gates, J.A. *Surf. Sci.* **1984**, *138*, 464.
24. Stroschio, J.A.; Bare, S.R.; Ho, W. *Surf. Sci.* **1984**, *148*, 499.
25. Slavin, A.J.; Bent, B.E.; Kao, C-T.; Somorjai, G.A. *Surf. Sci.* submitted.
26. Koel, B.E.; Crowell, J.E.; Mate, C.M.; Somorjai, G.A. *J. Phys. Chem.* **1984**,

88, 1988.

27. Ogletree, D.F.; Van Hove, M.A.; Somorjai, G.A. *Surf. Sci.* **1987**, *183*, 1.
28. Van Hove, M.A.; Lin, R.F.; Somorjai, G.A. *J. Am. Chem. Soc.* **1986**, *108*, 2532.
29. Lin, R.F.; Blackman, G.S.; Van Hove, M.A.; Somorjai, G.A. *Acta Crystallographica B* in press.
30. (a) Ohtani, H.; Bent, B.E.; Mate, C.M.; Van Hove, M.A.; Somorjai, G.A. *Applied Surf. Sci.* in press. (b) Ohtani, H.; Van Hove, M.A.; Somorjai, G.A. in preparation.
31. Grassian, V.H.; Muetterties, E.L. *J. Phys. Chem.* **1987**, *91*, 389.
32. Gomez-Sal, M.P.; Johnson, B.F.G.; Lewis, J.; Raithby, P.R.; Wright, A.H. *J. Chem. Soc., Chem. Comm.* **1985**, 1682.
33. Mate, C.M.; Somorjai, G.A. *Surf. Sci.* **1985**, *160*, 542.
34. Bertel, E.; Rosina, G.; Netzer, F. *Surf. Sci.* **1986**, *172*, L515.
35. Ohtani, H.; Wilson, R.J.; Chiang, S.; Mate, C.M. *Phys. Rev. Lett.* **1988**, *60*, 2398.
36. Koel, B.E.; Crowell, J.E.; Bent, B.E.; Mate, C.M.; Somorjai, G.A. *J. Phys. Chem.* **1986**, *90*, 2709.
37. (a) Gentle, T.M.; Muetterties, E.L. *J. Phys. Chem.* **1983**, *87*, 2469. (b) Sesselmann, W.; Woratschek, B.; Ertl, G.; Kupperts, J.; Haberland, H. *Surf. Sci.* **1983**, *130*, 245. (c) Tysoe, W.T.; Nyberg, G.L.; Lambert, R.M. *J. Chem. Soc., Chem. Comm.* **1983**, 623. (d) Tysoe, W.T.; Nyberg, G.L.; Lambert, R.M. *Surf. Sci.* **1983**, *135*, 128. (e) Rucker, T.G.; Logan M.A.; Gentle, T.M.; Muetterties, E.L.; Somorjai, G.A. *J. Phys. Chem.* **1986**, *90*, 2703. (f) Marchon, B. *Surf. Sci.* **1985**, *162*, 382.

38. Janowicz, A.H.; Bergman, R.G. *J. Am. Chem. Soc.* **1983**, *105*, 3929, and references therein.
39. While the explanations here are qualitative, it should be noted that a number of molecular orbital calculations on the structure and reactivity of surface hydrocarbon fragments have been published, including: (a) Kang, D.B.; Anderson, A.B. *Surf. Sci.* **1985**, *155*, 639, (b) Gavezzotti, A.; Simonetta, M. *J. Mol. Structure* **1984**, *107*, 75; *Surf. Sci.* **1980**, *99*, 453. (c) Minot, C.; Van Hove, M.A.; Somorjai, G.A. *Surf. Sci.* **1982**, *127*, 441. (d) Silvestre, J.; Hoffmann, R. *Langmuir* **1985**, *1*, 621. (e) Zheng, C.; Apeloig, Y.; Hoffmann, R. *J. Am. Chem. Soc.* **1988**, *110*, 749.
40. Somorjai, G.A. *Chemistry in Two Dimensions: Surfaces*; Cornell Univ. Press: Ithaca, 1981.
41. Muetterties, E.L. *Chem. Soc. Rev.* **1982**, *11*, 283.
42. Collman, J.P.; Hegedus, L.S. *Principles and Applications of Organotransition Metal Chemistry*; University Science Books: Mill Valley, 1980.
43. Muetterties, E.L. in "Reactivity of Metal-Metal Bonds", ACS Symposium Series No. 155, M.H. Chisholm, ed., 1981, 273.
44. Muetterties, E.L. *Angew. Chem. Int. Ed. Engl.* **1978**, *17*, 545.
45. Low preexponential factors could also reflect decomposition at a small number of surface defects.
46. Salmeron, M.; Somorjai, G.A. *J. Phys. Chem.* **1982**, *80*, 341.
47. Hall, R.B.; DeSantolo, A.M.; Bare, S.J. *Surf. Sci.* **1985**, *161*, L533.
48. Gates, S.M.; Russell, Jr., J.N.; Yates, Jr., J.T. *Surf. Sci.* **1986**, *171*, 111.
49. McCabe, R.W.; DiMaggio, C.L.; Madix, R.J. *J. Phys. Chem.* **1985**, *89*, 854.

50. Godbey, D.; Zaera, F.; Yeates, R.; Somorjai, G.A. *Surf. Sci.* **1986**, *167*, 150.
51. Somorjai, G.A.; Van Hove, M.A.; Bent, B.E. *J. Phys. Chem.* **1988**, *92*, 973.
52. Bradshaw, A.M.; Hoffmann, F.M. *Surf. Sci.* **1978**, *72*, 513.
53. Van Hove, M.A.; Koestner, R.J.; Frost, J.C.; Somorjai, G.A. *Surf. Sci.* **1983**, *129*, 482.
54. Crowell, J.E.; Tysoe, W.T.; Somorjai, G.A. *J. Phys. Chem.* **1985**, *89*, 1598.
55. Mate, C.M.; Kao, C-T.; Somorjai, G.A. *Surf. Sci.* submitted.
56. White, J.M. *J. Vac. Sci. Technol. A*, in press, and references therein.
57. Slavin, A.J.; Bent, B.E.; Kao, C-T.; Somorjai, G.A. *Surf. Sci.* submitted.
58. (a) Cabrera, A.L.; Spencer, N.D.; Kozak, E.; Davies, P.W.; Somorjai, G.A. *Rev. Sci. Instrum.* **1982**, *53*, 1888. (b) Blakely, D.W.; Kozak, E.I.; Sexton, B.A.; Somorjai, G.A. *J. Vac. Sci. Technol.* **1976**, *13*, 1091.
59. Horiuti, J.; Miyahara, K. "Hydrogenation Over Metallic Catalysts" NSRDS-NBS-13, 1969.
60. Zaera, F.; Somorjai, G.A. *J. Am. Chem. Soc.* **1984**, *106*, 2288.
61. Wieckowski, A.; Rosasco, S.D.; Salaita, G.N.; Hubbard, A.; Bent, B.E.; Zaera, F.; Godbey, D.; Somorjai, G.A. *J. Am. Chem. Soc.* **1985**, *107*, 5910.
62. Davis, S.M.; Zaera, F.; Gordon, B.E.; Somorjai, G.A. *J. Catal.* **1985**, *92*, 240.
63. Beebe, Jr., T.P.; Yates, Jr., J.T. *J. Am. Chem. Soc.* **1986**, *108*, 663.
64. Davis, S.M.; Somorjai, G.A. *Bull. Soc. Chim. Fran.* **1985**, 271.

65. (a) Gillespie, W.D.; Herz, R.K.; Petersen, E.E.; Somorjai, G.A. *J. Catal.* **1981**, *70*, 147. (b) Davis, S.M.; Zaera, F.; Somorjai, G.A. *J. Catal.* **1984**, *85*, 206.
66. Davis, S.M.; Zaera, F.; Somorjai, G.A. *J. Am. Chem. Soc.* **1982**, *104*, 7453.
67. Davis, S.M.; Zaera, F.; Somorjai, G.A. *J. Catal.* **1982**, *77*, 439.
68. Fersht, A. *Enzyme Structure and Mechanism*; W.H. Freeman: San Francisco, 1977, Chapter 10.
69. Bent, B.E.; Nuzzo, R.G.; Dubois, L.H. *J. Am. Chem. Soc.* submitted.
70. (a) Hubbard, A.T. *Acc. Chem. Res.* **1980**, *13*, 177. (b) Hubbard, A.T.; Stickney, J.L.; Rosasco, S.D.; Soriaga, M.P.; Song, D. *J. Electroanal. Chem.* **1983**, *150*, 165.
71. (a) Sonnenfeld, R.; Hansma, P.K. *Science* **1986**, *232*, 211. (b) Sonnenfeld, R.; Schardt, B.C. *Appl. Phys. Lett.* **1986**, *49*, 1172.
72. Shen, Y.R. *The Principles of Nonlinear Optics*; John Wiley: New York, 1984.

Figure Captions

Figure 1: (A) Schematic diagram of an ultra-high vacuum apparatus for surface analysis by low energy electron diffraction (LEED), Auger electron spectroscopy (AES), and high resolution electron energy loss spectroscopy (HREELS). The mass spectrometer is for thermal desorption studies. The manipulator is shown extended to position the sample in the HREEL spectrometer. This particular apparatus also includes a high pressure cell tube (which can be extended and sealed around the single crystal sample as shown in (B)) and an external reaction loop for studies of catalytic reactions over the single crystal sample at one atmosphere pressure.

Figure 2: Structure of several surfaces of a face-centered cubic (fcc) metal. The low Miller index (111) and (100) surfaces are both nominally flat, but have hexagonal and square arrangements of the surface atoms respectively. The high Miller index (755) and (10,8,7) surfaces have (111) terraces with periodic steps and kinks.

Figure 3: Principles of high-resolution electron energy loss spectroscopy (HREELS) as applied to a (2x2) monolayer of ethylidyne (CCH_3) on Rh(111): (A) the experiment, (B) the spectrum, (C) the phenomena responsible for the dipole selection rule, and (D) the spectral assignment for ethylidyne.

Figure 4: Outline of the steps involved in solving an adsorbate surface structure by low energy electron diffraction (LEED) using the (2x2) structure of ethylidyne (CCH_3) on Rh(111) as an example.

Figure 5: Hydrogen thermal desorption from monolayers of the indicated alkenes adsorbed on a Rh(111) surface cooled to less than 100K. The surface heating rates were 15-20 K/sec.

Figure 6: High resolution electron energy loss vibrational spectra (taken in the specular direction) and proposed surface bonding geometries for the stable surface fragments formed during the thermal

decomposition of an ethylene monolayer on a Rh(111) surface. The spectra were recorded after annealing to the indicated temperatures.

Figure 7: The Dewar-Chat-Duncanson model of ethylene coordination to transition metal surfaces. Diagrams A and B show the interaction of the ethylene highest occupied (π) and lowest unoccupied (π^*) molecular orbitals with filled and empty metal surface orbitals respectively. Diagrams C and D depict, using valence bond formalism, the resulting extremes (π and $\text{di-}\sigma$) in bonding to the surface.

Figure 8: Comparison of bond lengths and bond angles in surface- and cluster-bound ethylidyne species. Corresponding parameters for acetylene, ethylene and ethane are also given for comparison.

Figure 9: Comparison of the different types of alkylidyne coordination that are known for organometallic complexes. Not shown, but reported in the literature [20], is a 4-fold coordinated CCH_3 ligand bonded to an Os_6 cluster.

Figure 10: Cluster bonding geometries known for the CH ligand in organometallic chemistry along with the proposed CH bonding geometry on a Rh(111) surface.

Figure 11: Cluster bonding geometries known for the C_2H ligand in organometallic chemistry along with the proposed C_2H bonding geometries on Rh(111) and Rh(100).

Figure 12: Pathways for the thermal decomposition of ethylene, propylene, methylacetylene, and propadiene on a Rh(111) surface. These decomposition intermediates, determined by surface vibrational spectroscopy and thermal desorption studies using isotope labeling, are stable in the indicated temperature ranges.

Figure 13: High resolution electron energy loss surface vibrational spectra for

monolayers of benzene adsorbed on the indicated surfaces at 300K. At this temperature, benzene is molecularly adsorbed on all three surfaces, bonding with its π ring parallel to the surface plane.

Figure 14: Top views of the arrangement of CO and benzene in the unit cell of the indicated coadsorption structures on the Pt(111) and Rh(111) surfaces. As determined by HREELS, benzene is oriented with its π ring parallel to the surface and CO (hatched circles) is bonded with its molecular axis perpendicular to the surface, carbon end down. Gas phase Van der Waals dimensions are shown.

Figure 15: Carbon-carbon bond lengths determined by LEED for benzene adsorption on a Rh(111) surface (coadsorbed with a stoichiometric amount of carbon monoxide) [28,29] and determined by x-ray crystallography for benzene bonding in a triruthenium organometallic cluster [32]. Both on the surface and in the cluster the benzene coordinates to three metal atoms and shows a 3-fold symmetric distortion resulting in alternating long and short C-C bonds.

Figure 16: Hydrogen thermal desorption from benzene (top curve) and ethylene (bottom curve) adsorbed on Rh(111), with schematic indication of the fragmentation pathways responsible for this hydrogen evolution.

Figure 17: Proposed scheme for ethylene fragmentation on transition metal surfaces in the absence of carbon-carbon bond breaking. All of the elementary steps are either hydrogenation (reductive elimination) or dehydrogenation (oxidative addition) reactions.

Figure 18: Schematic representation of the surface intermediates and energetics for the previously postulated dehydrogenation/hydrogenation mechanism and for the newly proposed hydrogenation/dehydrogenation mechanism for ethyli-

dyne formation on transition metal surfaces. (*) = energetics based on molecular orbital calculations for a Pt(111) surface [39a]; (#) = energetics from experimental measurement and modelling of ethylene hydrogenation to ethane on a Pt(111) surface [50].

Figure 19: Isosteric heat of adsorption for carbon monoxide on the Pd(111) crystal face as a function of surface coverage. (After Conrad, H.; Ertl, G.; Koch, J.; Latta, E.E. *Surf. Sci.* **1974**, *43*, 462.)

Figure 20: Surface structure determined by low energy electron diffraction for a saturation coverage of carbon monoxide on Rh(111). Top and side views are shown. Large circles represent Rh atoms, while smaller circles correspond to C and O atoms. Solid lines show the structure expected for hexagonal close-packing of the carbon monoxide, while dotted circles depict the actual structure.

Figure 21: Carbon monoxide dissociation on a Rh(111) surface as a function of potassium coverage. Thermal desorption isotope scrambling experiments using $^{13}\text{C}^{16}\text{O}$ and $^{12}\text{C}^{18}\text{O}$ were performed to monitor this chemistry.

Figure 22: Top views of Rh(111) surfaces showing the effects of temperature and CO on the ordering of a quarter monolayer of ethylidyne (CCH_3) species. The bonding sites and geometries for both of the ordered structures have been determined by low energy electron diffraction surface crystallography.

Figure 23: Comparison of the thermal fragmentation pathways for ethylene adsorbed with and without CO on the Rh(111) and Rh(100) surfaces.

Figure 24: Evidence for the presence of ethylidyne (CCH_3) on the Rh(111) surface after ethylene hydrogenation at atmospheric pressure over this surface. High-resolution electron energy loss spectroscopy (HREELS), low energy electron diffraction (LEED), and thermal desorption spectroscopy (TDS) data for ethylidyne are compared

with the results of these techniques on Rh(111) after catalytic ethylene hydrogenation and transfer of the crystal to ultra-high vacuum. The differences in the LEED patterns are due to the increased amount of coadsorbed carbon monoxide on the surface after reaction (see Fig. 22).

- Figure 25: Comparison of the rates of catalytic ethylene hydrogenation, ethylidyne rehydrogenation and ethylidyne H,D-exchange over Pt(111) and Rh(111) surfaces as measured by gas chromatography, radio tracer studies, and surface vibrational spectroscopy respectively. These rates show that ethylidyne cannot be an intermediate in the catalytic hydrogenation of ethylene over these surfaces at room temperature.
- Figure 26: Mechanisms proposed for the catalytic hydrogenation of ethylene over Pt(111) and Rh(111) surfaces at 300K and at high pressure.
- Figure 27: Skeletal rearrangement reactions of n-hexane catalyzed by platinum surfaces with high activity and unique selectivity. These hydrocarbon conversion reactions are illustrative of those that occur simultaneously during the production of high octane gasoline from petroleum naphtha.
- Figure 28: Dehydrocyclization of alkanes to aromatic hydrocarbons is one of the most important petroleum reforming reactions. The bar graphs here compare reaction rates for n-hexane and n-heptane aromatization catalyzed at 573K and atmospheric pressures over two flat platinum single crystal surfaces with different atomic structure. The (111) surface with the hexagonal atomic arrangement is several times more active over a wide range of reaction conditions than the (100) surface having a square unit cell.
- Figure 29: Reaction rates are shown as a function of surface structure for isobutane isomerization and hydrogenolysis catalyzed at 570K and atmospheric pressures over four platinum surfaces. The rates for both reaction pathways are quite sensitive to the structural

features of these single crystal model catalyst surfaces. Isomerization of this light alkane is most favored on the platinum (100) surface having a square unit cell, while hydrogenolysis rates are maximized when kink sites are present at high concentrations as on the platinum (10,8,7) crystal surface.

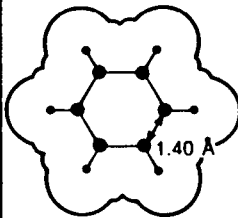
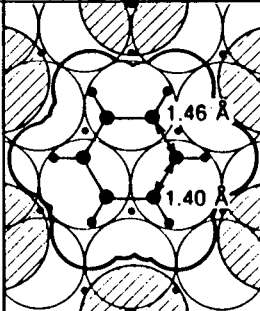
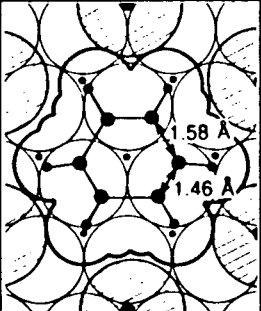
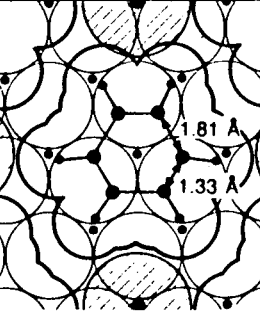
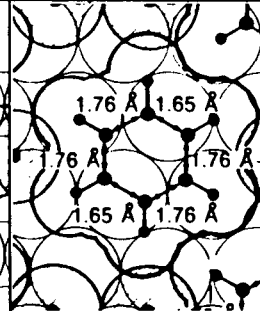
Figure 30: Hydrocarbon fragment stoichiometry and the fraction of irreversibly adsorbed carbon on a Pt(111) surface after adsorption of ethylene at temperatures between 100 and 400C. Carbon-14 labelled ethylene was used to determine the the amount of irreversibly adsorbed carbon after heating the adsorbed monolayer in 1 atmosphere of hydrogen at the adsorption temperature. The irreversibly adsorbed species have surface residence times on the order of days. The H/C composition of the adsorbed monolayer was determined from thermal desorption studies.

TABLE I

Table of surface characterization techniques that are used to determine the structure and composition of solid surfaces. Adsorbed species present at concentrations of 1% of a monolayer can be readily detected.

<u>SURFACE ANALYSIS METHOD</u>	<u>ACRONYM</u>	<u>PHYSICAL BASIS</u>	<u>TYPE OF INFORMATION OBTAINED</u>
Low energy electron diffraction	LEED	Elastic backscattering low energy electrons	Atomic surface structure of surfaces and of adsorbed gases
Auger electron spectroscopy	AES	Electron emission from surface atoms excited by electron x-ray or ion bombardment	Surface composition
High resolution electron energy loss spectroscopy	HREELS	Vibrational excitation of surface atoms by inelastic reflection of low energy electrons	Structure and bonding of surface atoms and adsorbed species.
Infrared spectroscopy	IRS	Vibrational excitation of surface atoms by adsorption of infrared radiation.	Structure and bonding of adsorbed gases.
X-ray and ultraviolet photoelectron spectroscopy	XPS UPS	Electron emission from atoms	Electronic structure and oxidation state of surface atoms and adsorbed species.
Ion scattering spectroscopy	ISS	Inelastic reflection of inert gas ions.	Atomic structure and composition of solid surfaces
Secondary ion mass spectroscopy	SIMS	Ion beam induced ejection of surface atoms as positive & negative ions	Surface composition
Extended X-ray absorption fine structure analysis	EXAFS	Interference effects during x-ray emission	Atomic structure energetics composition of adsorbed species
Thermal desorption spectroscopy	TDS	Thermally induced desorption or decomposition of adsorbed species	Adsorption energetics composition of adsorbed species
Solid state nuclear magnetic resonance	Solid-state NMR	Nuclear magnetic resonance on samples with areas of 1 m ² or larger	Atomic and molecular composition, structure

Table II

Substrate	(Gas Phase)	Pd(111)	Rh(111)		Pt(111)
Surface Structure		(3x3)-C ₆ H ₆ + 2CO	(3x3)-C ₆ H ₆ + 2CO	c(2√3x4)rect-C ₆ H ₆ + CO	(2√3x4)rect-2C ₆ H ₆ + 4CO
The Structure of Benzene					
C ₆ Ring Radius (Å)	1.40	1.43±0.10	1.51±0.15	1.65±0.15	1.72±0.15
d _{M-C} (Å)	-	2.39±0.05	2.30±0.05	2.35±0.05	2.25±0.05
γ _{CH} (cm ⁻¹) ^a	670	720-770	780-810		830-850

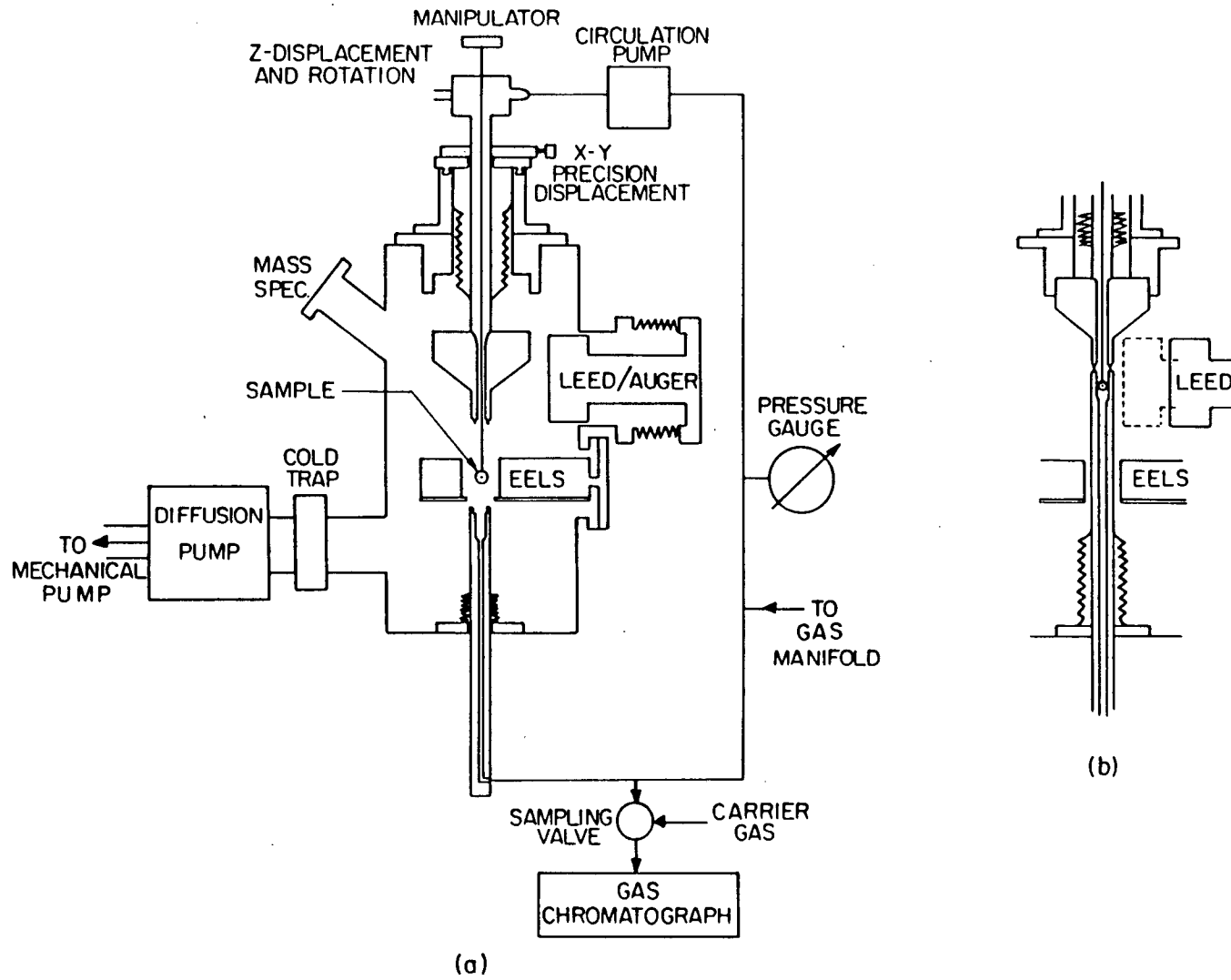
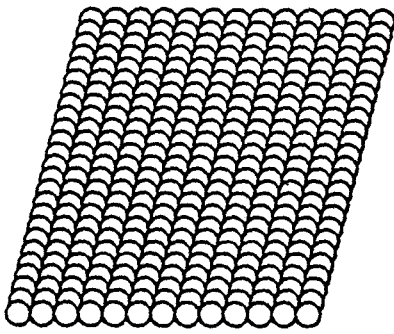
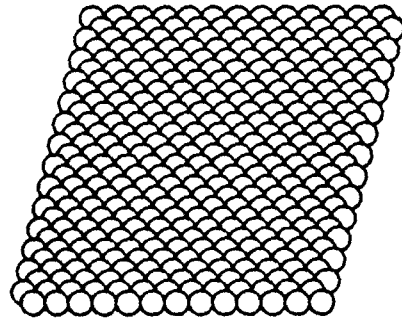


Fig. 1

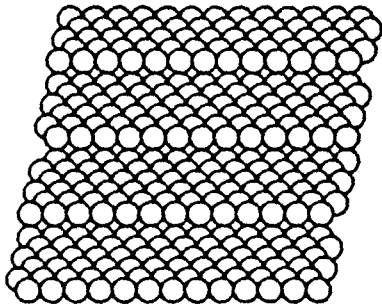
XBL 8111-6950



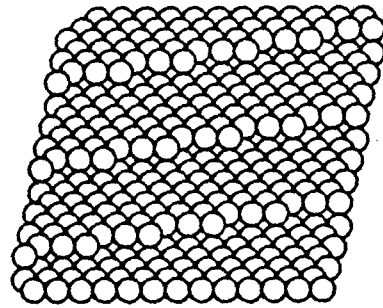
fcc (100)



fcc (111)



fcc (110)



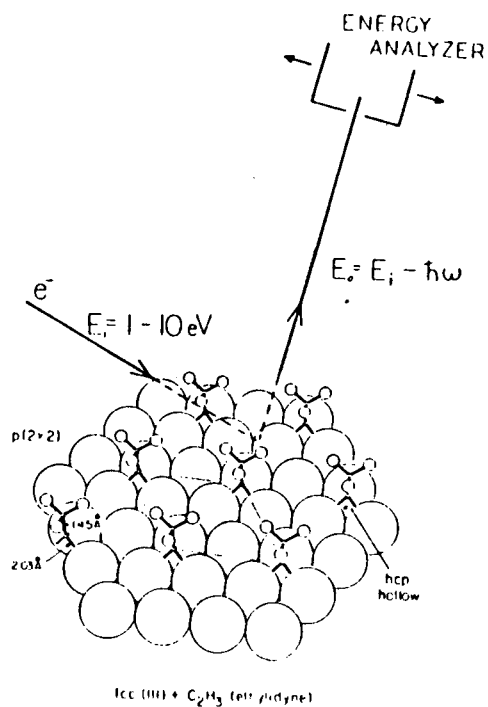
fcc (100)

XBL 8112-13009

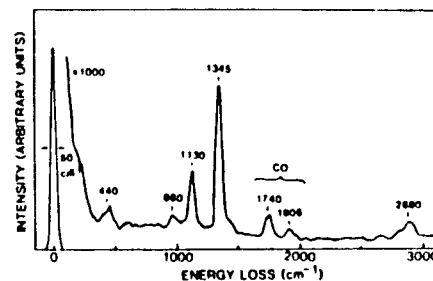
Fig. 2

High Resolution Electron Energy Loss Spectroscopy (HREELS): Ethyldiyne on Rh(III)

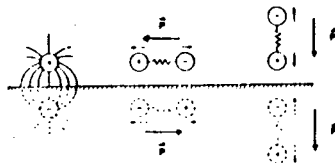
(A) Electron Scattering



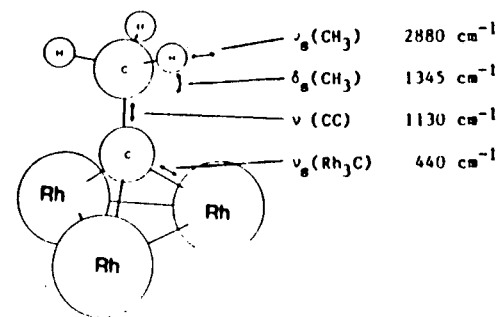
(B) HREEL Vibrational Spectrum



(C) The Dipole Selection rule



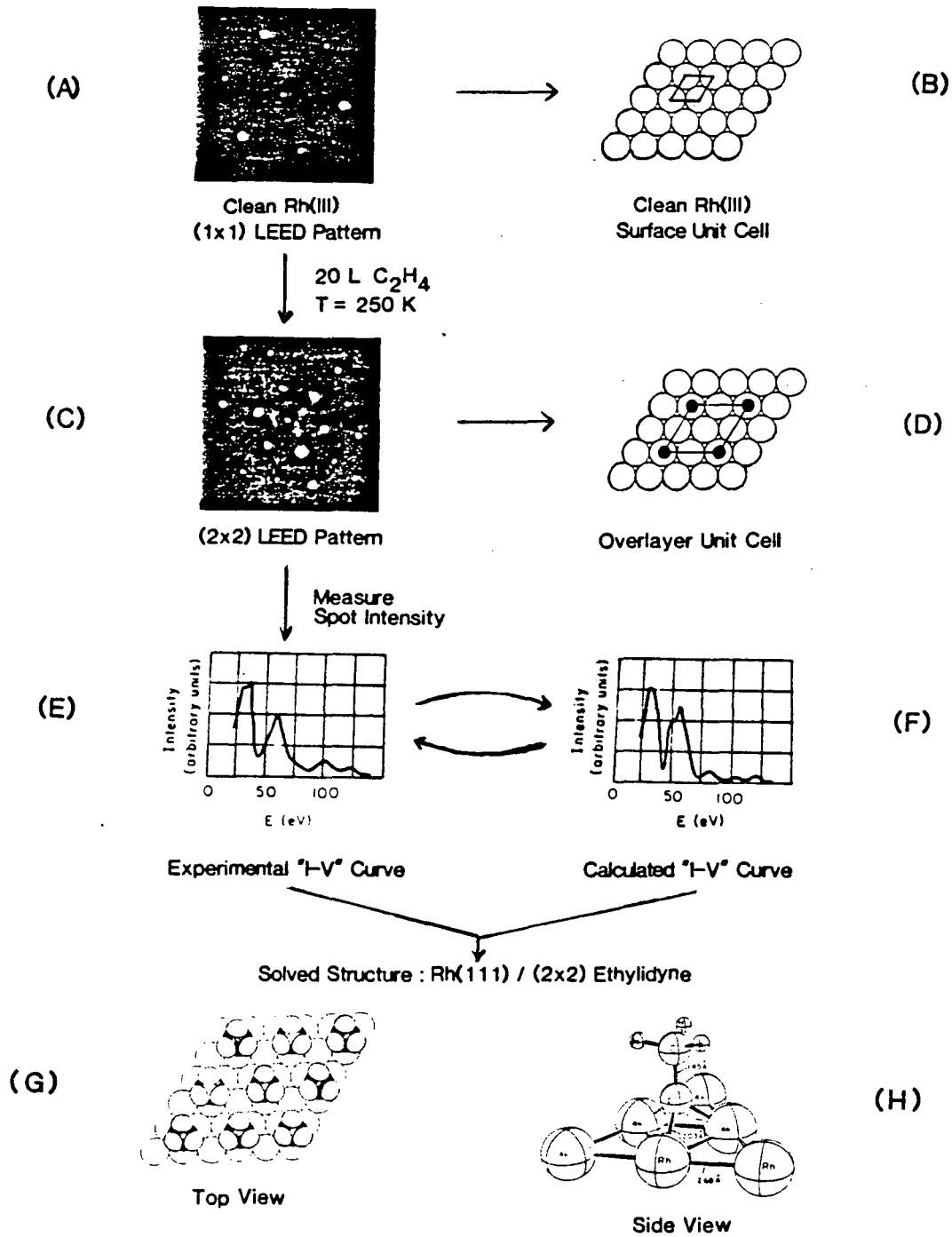
(D) Spectral Assignment



XBL 8610-4095

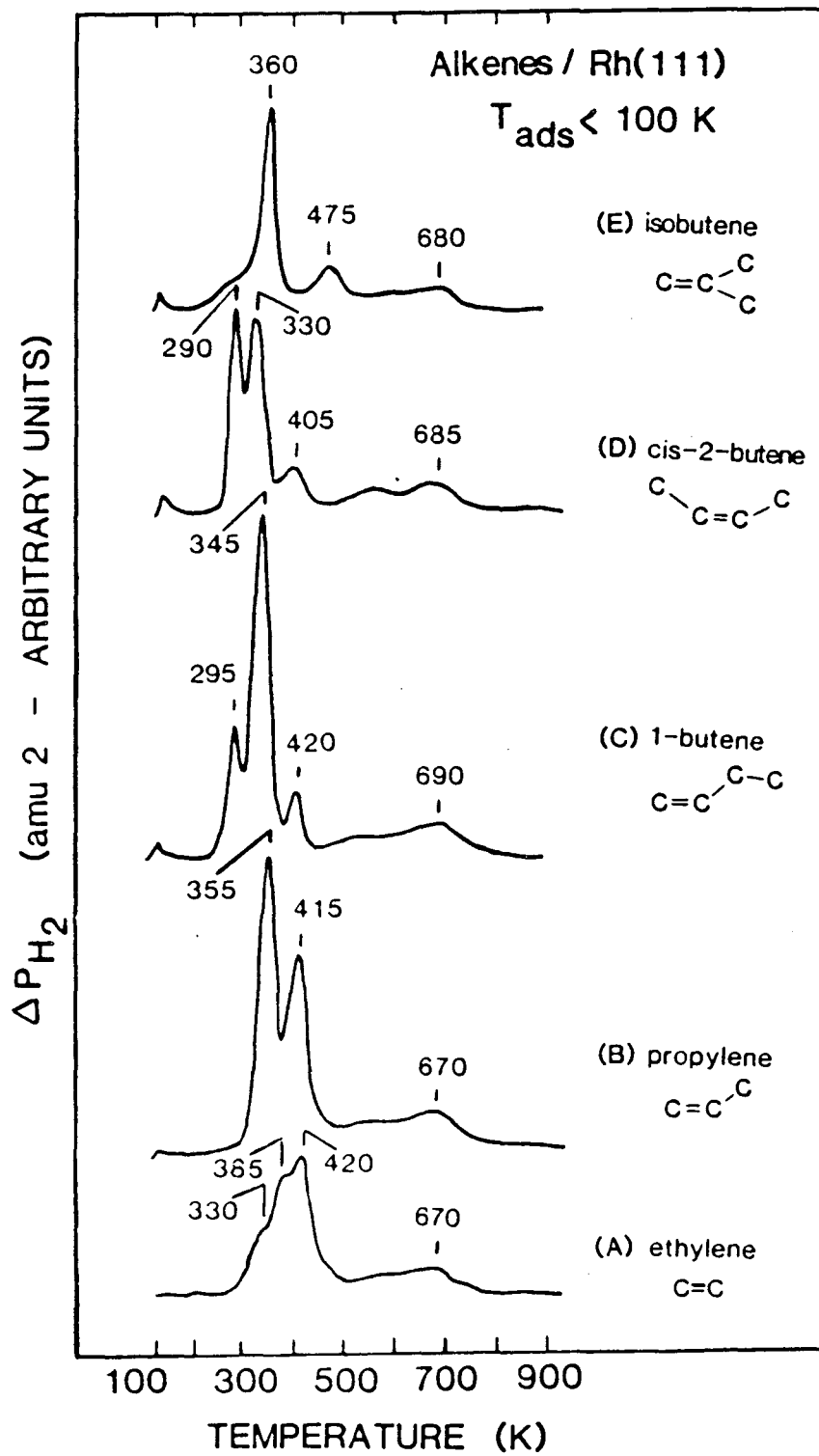
Fig. 3

Steps to a Solved Surface Structure by LEED : Ethylidyne on Rh(III)



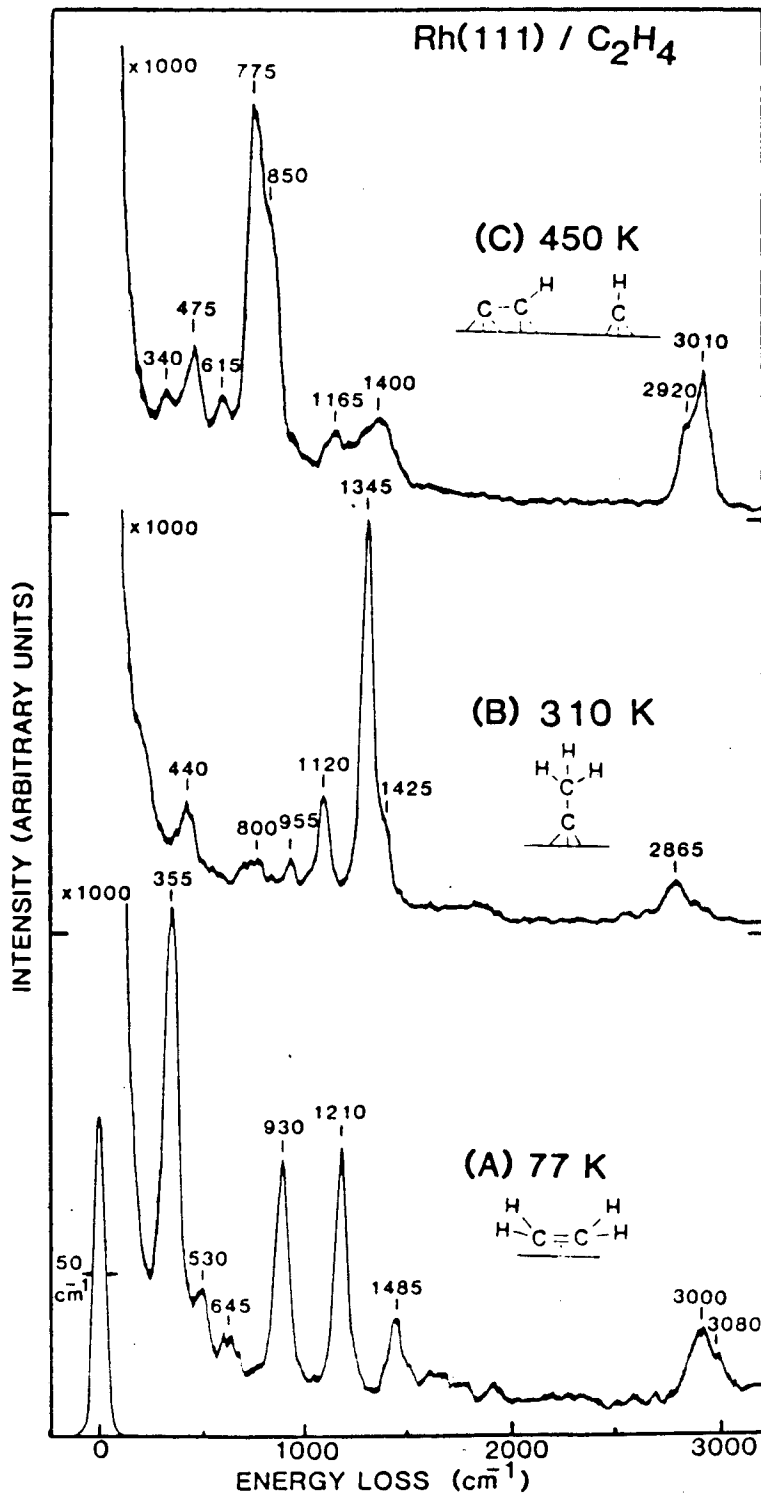
XBL 8610-4097

Fig. 4



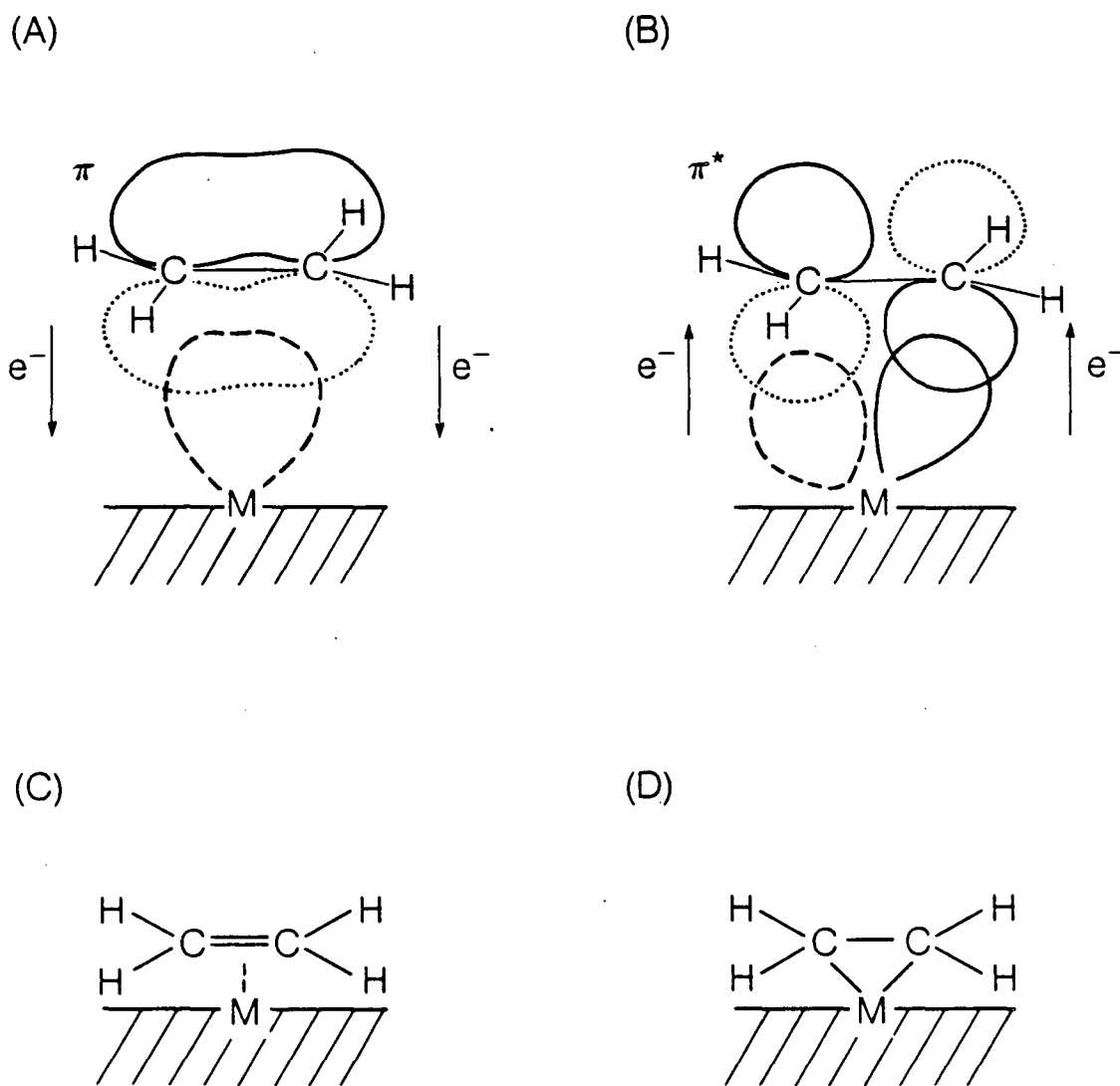
XBL 868-3195

Fig. 5



XBL 8512-4941

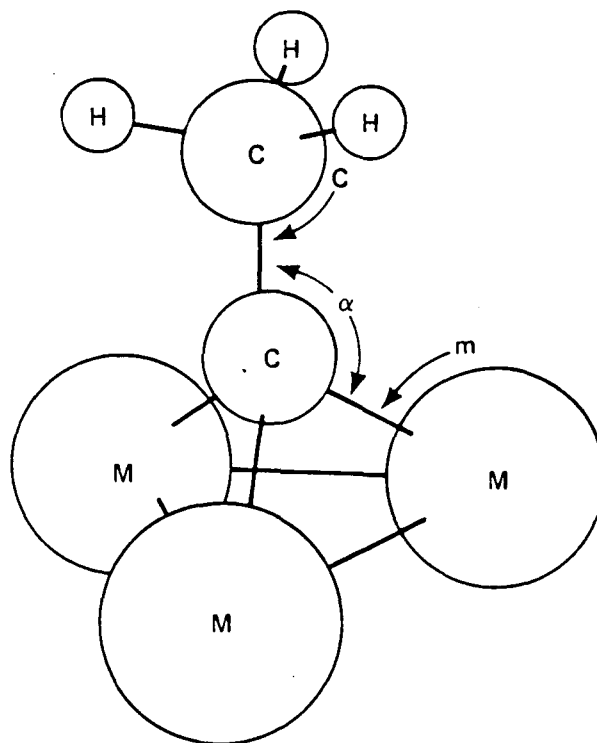
Fig. 6



XBL 866-11177

Fig. 7

Different ethynyl species: bond distances and angles
 (r_C = carbon covalent radius; r_M = bulk metal atomic radius)

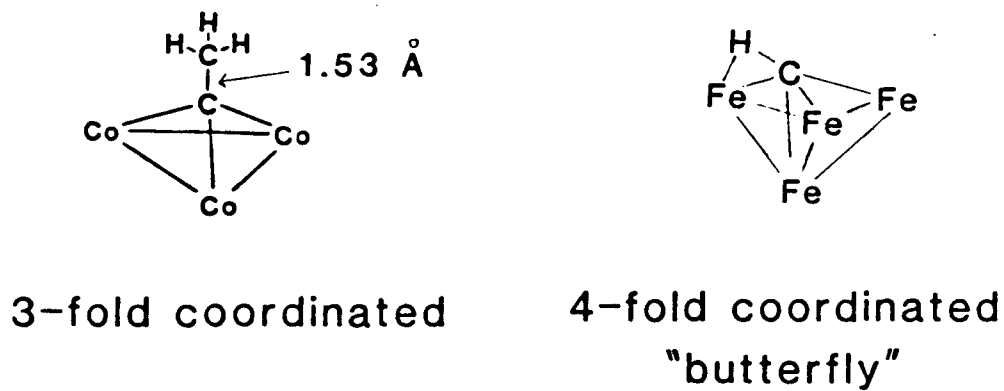
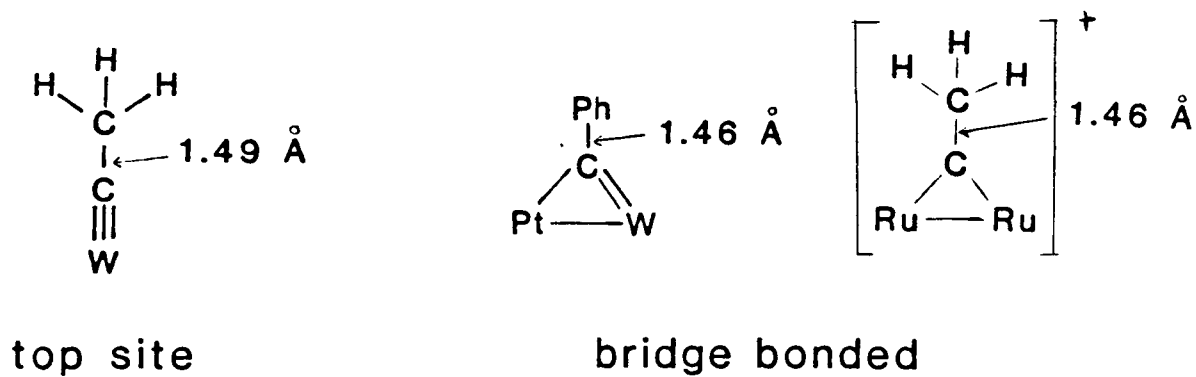


	C [Å]	m	r_M	r_C	α [°]
$\text{Co}_3 (\text{CO})_9 \text{CCH}_3$	1.53 (3)	1.90 (2)	1.25	0.65	131.3
$\text{H}_3 \text{Ru}_3 (\text{CO})_9 \text{CCH}_3$	1.51 (2)	2.08 (1)	1.34	0.74	128.1
$\text{H}_3 \text{Os}_3 (\text{CO})_9 \text{CCH}_3$	1.51 (2)	2.08 (1)	1.35	0.73	128.1
$\text{Pt}^\dagger (111) + (2 \times 2) \text{CCH}_3$	1.50	2.00	1.39	0.61	127.0
$\text{Rh} (111) + (2 \times 2) \text{CCH}_3$	1.45 (10)	2.03 (7)	1.34	0.69	130.2
$\text{H}_3\text{C} - \text{CH}_3$	1.54			0.77	109.5
$\text{H}_2\text{C} = \text{CH}_2$	1.33			0.68	122.3
$\text{HC} \equiv \text{CH}$	1.20			0.60	180.0

XBL 818-11196

Fig. 8

Alkylidyne Coordination in Organometallic Complexes

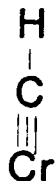
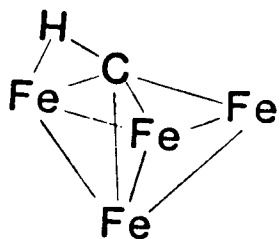
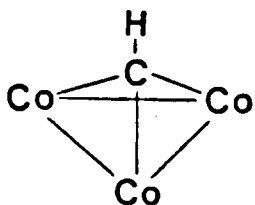


XBL 8610-4113

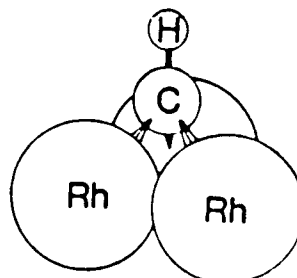
Fig. 9

Surface and Cluster Bonding of Methylidyne

Known Cluster
Coordination



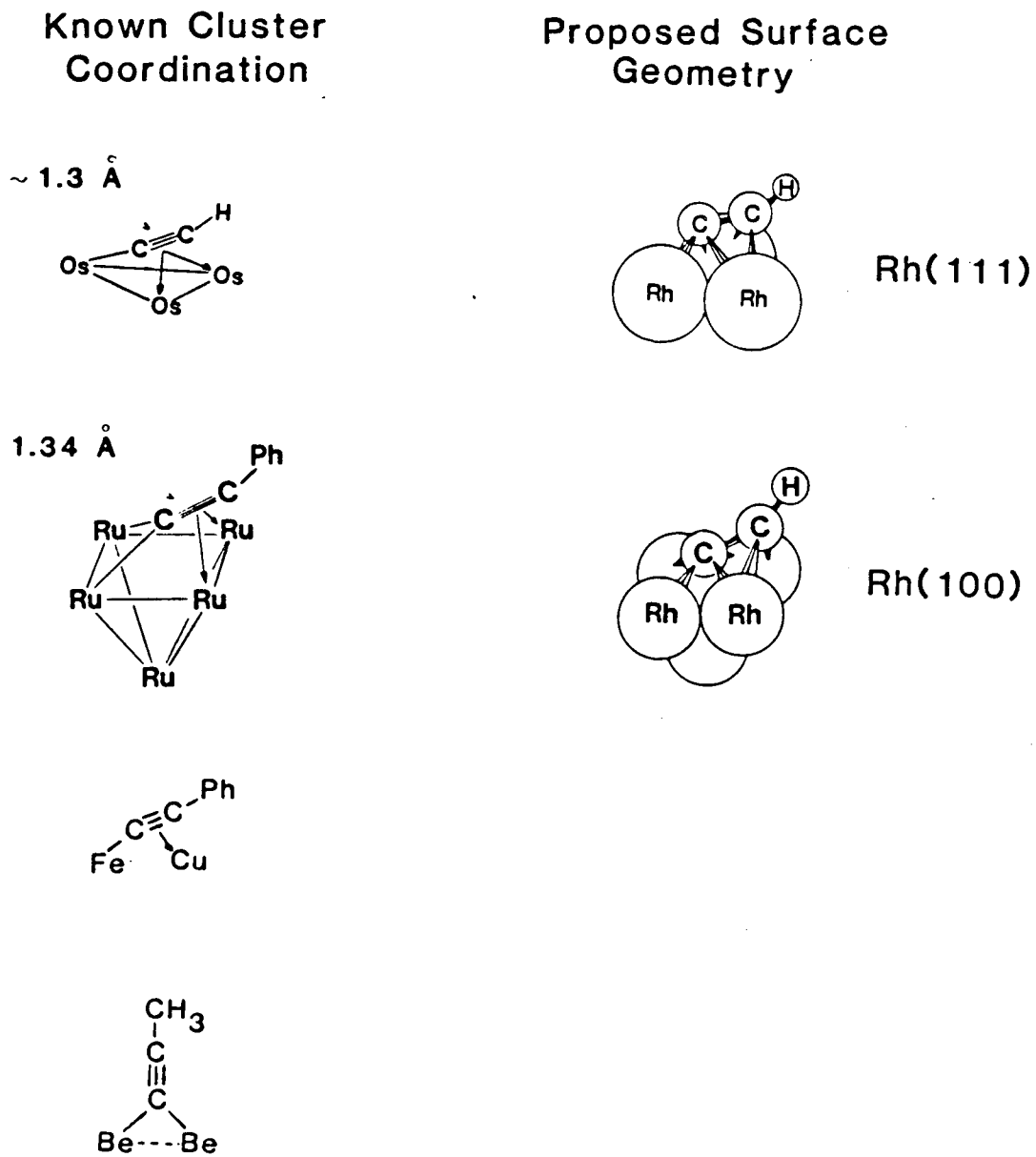
Proposed Surface Geometry
on Rh(111)



XBL 8610-4100

Fig. 10

Surface and Cluster Bonding of Acetylide

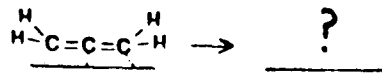


XBL 8610-4101

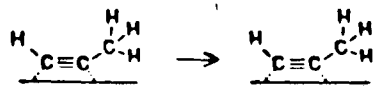
Fig. 11

Hydrocarbon Decomposition on Rh(111)

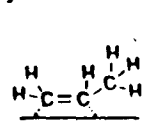
Propadiene



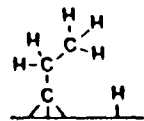
Methylacetylene



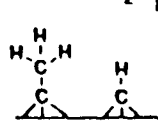
Propylene



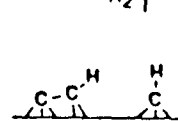
200K



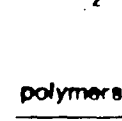
330K



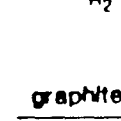
420K



530K



800K



Ethylene

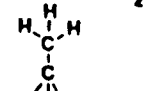
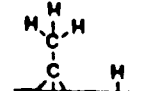
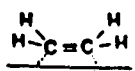
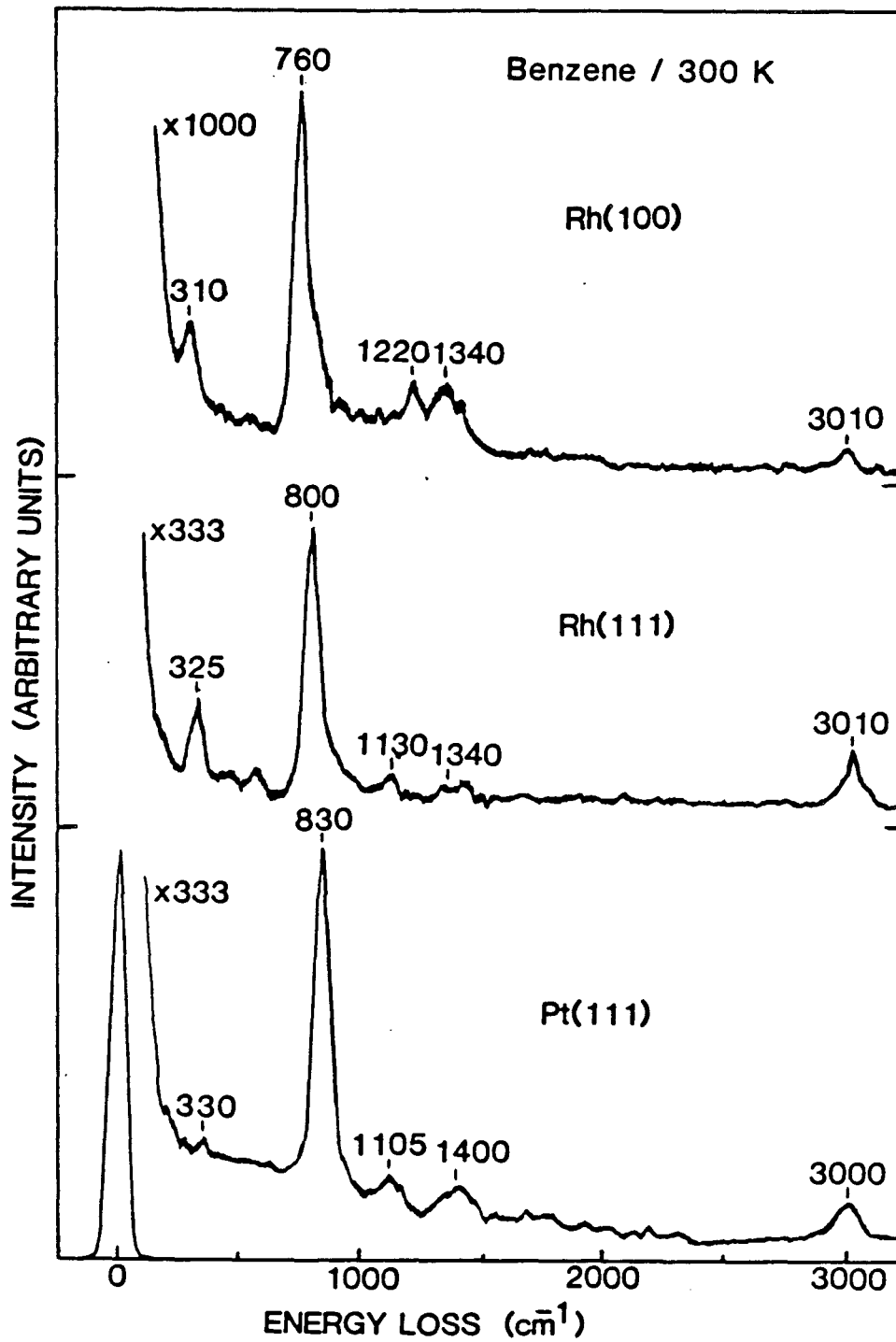
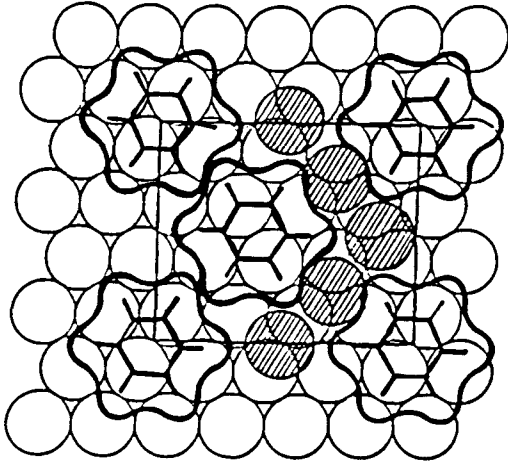
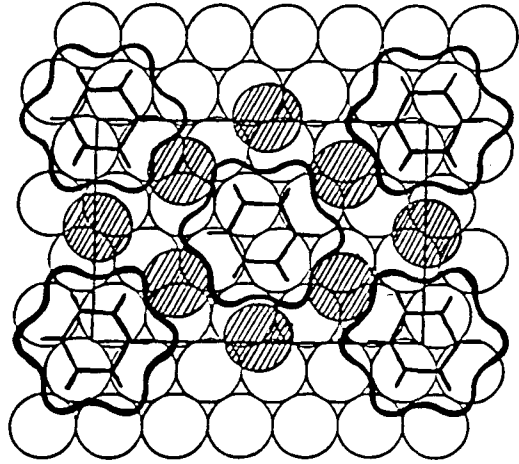
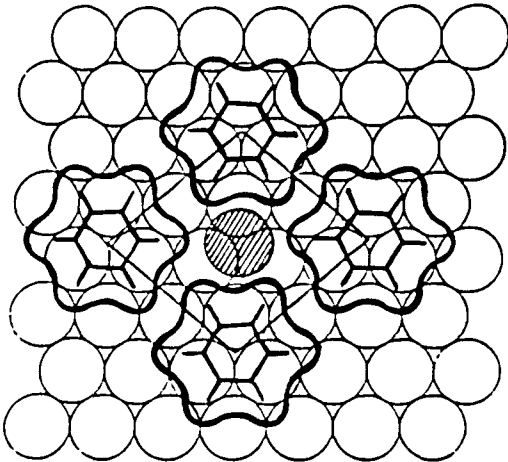
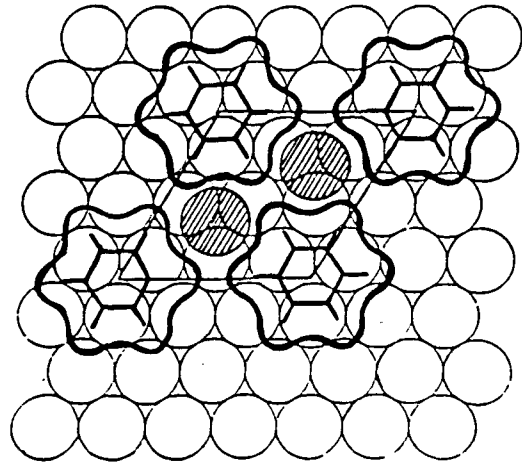


Fig. 12



XBL 8512-4938

Fig. 13

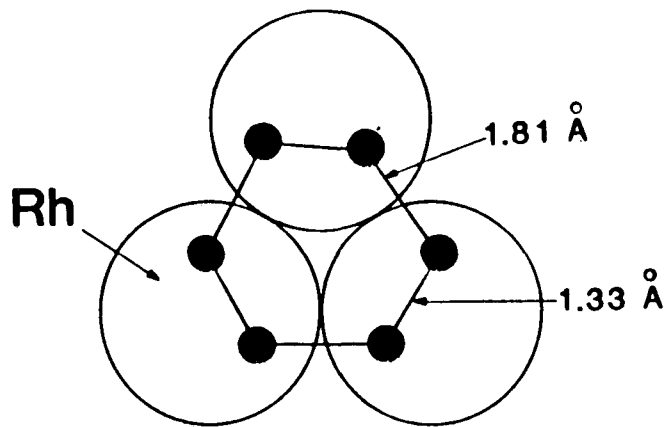
$\text{CO/C}_6\text{H}_6/\text{Pt (III)}$ (A) $(2\sqrt{3} \times 4)$ rect(B) $(2\sqrt{3} \times 5)$ rect $\text{CO/C}_6\text{H}_6/\text{Rh (III)}$ (C) $c(2\sqrt{3} \times 4)$ rect(D) (3×3) 

XBL 849-10795

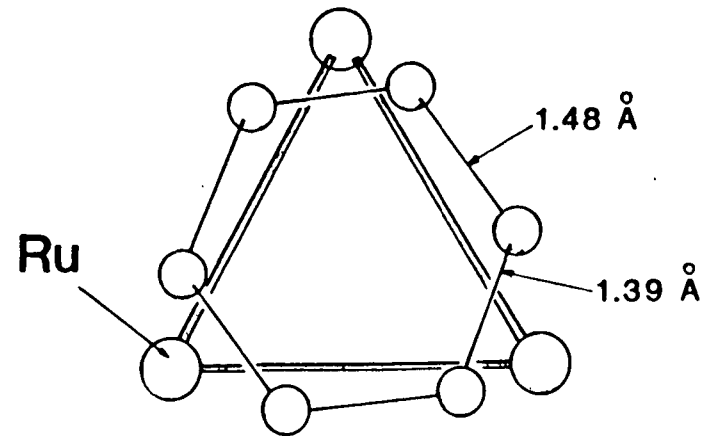
Fig. 14

Benzene Bonding Geometries

Surface



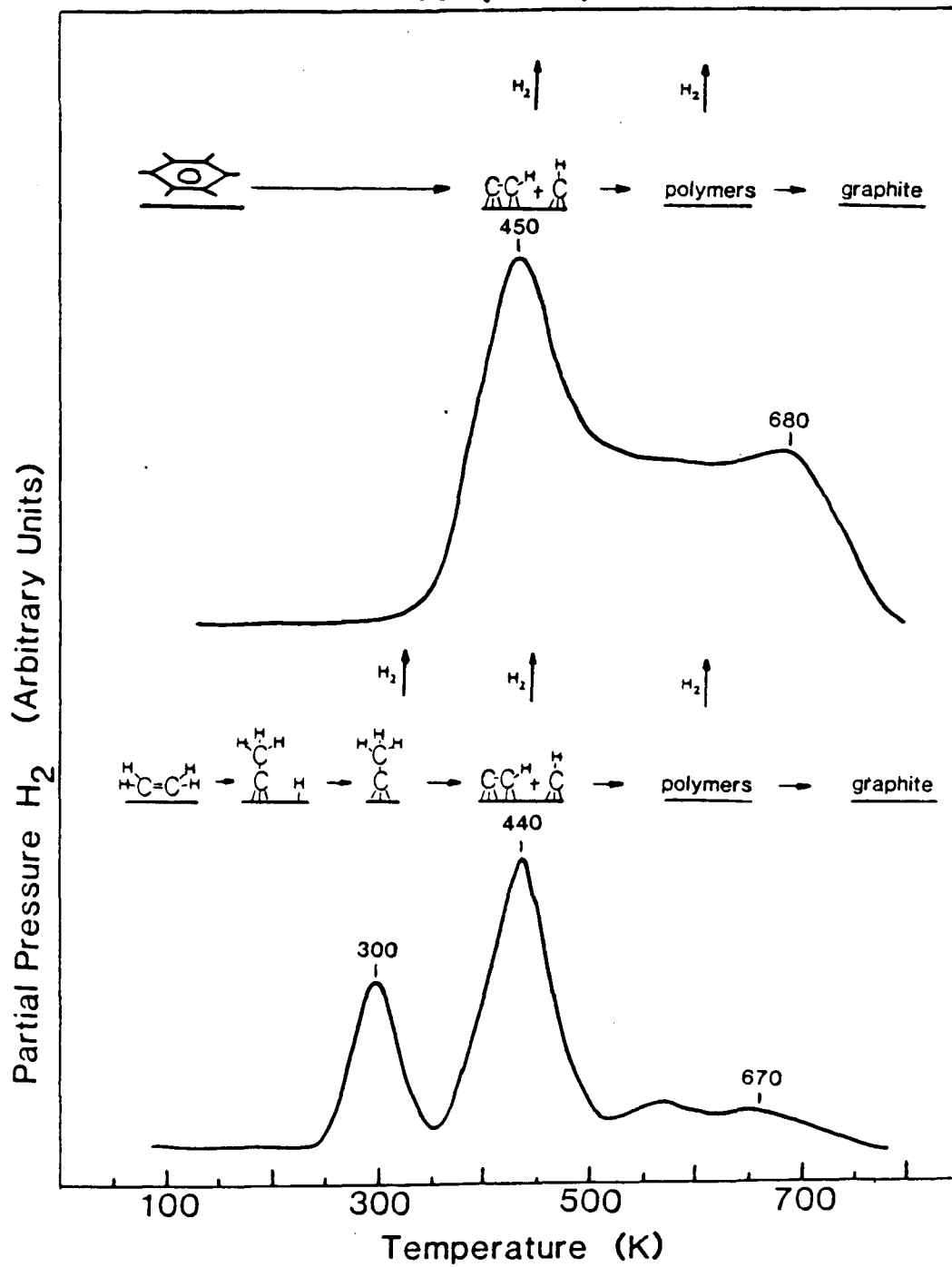
Cluster



XBL 8512-4939

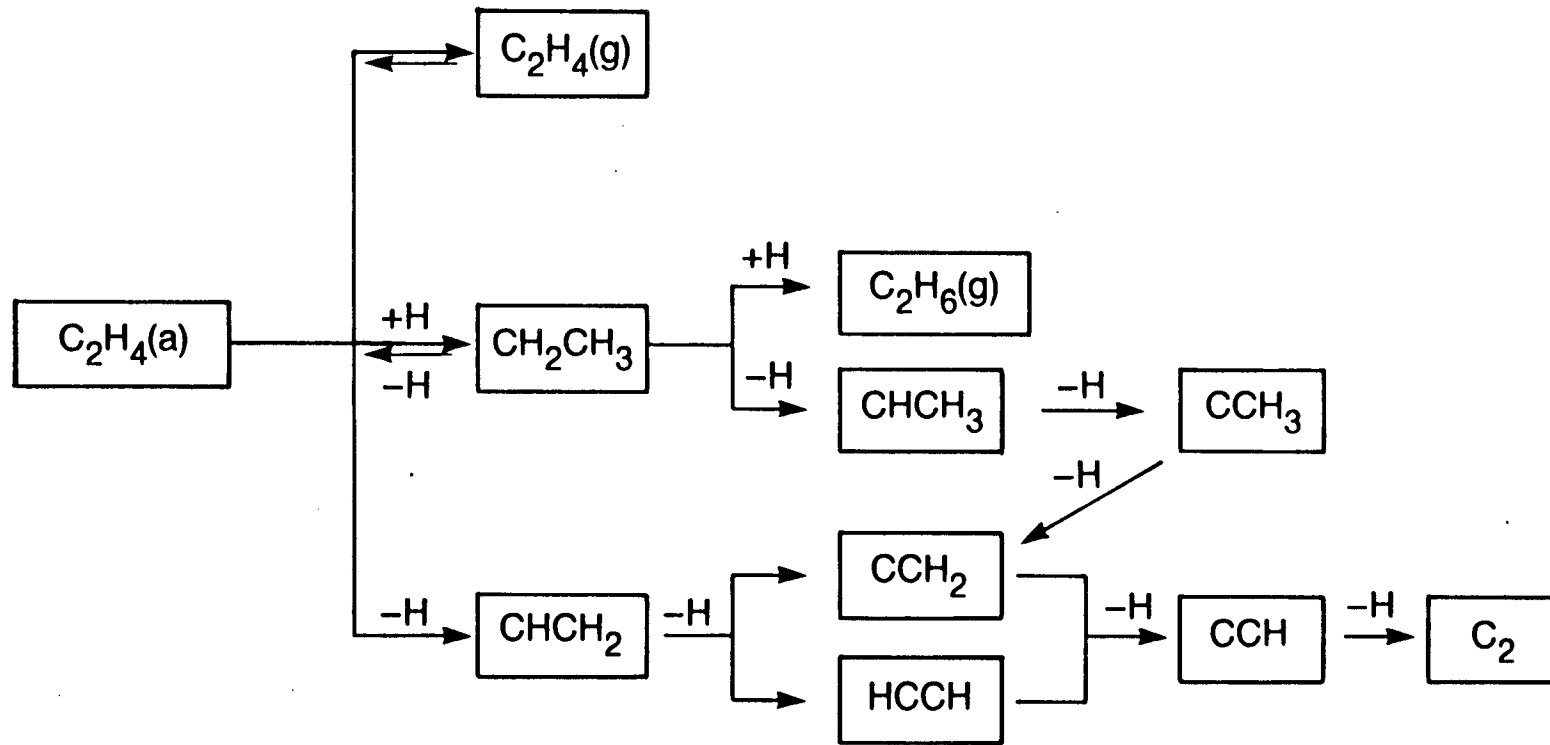
Fig. 15

Rh(111)



XBL 8512-4937

Fig. 16

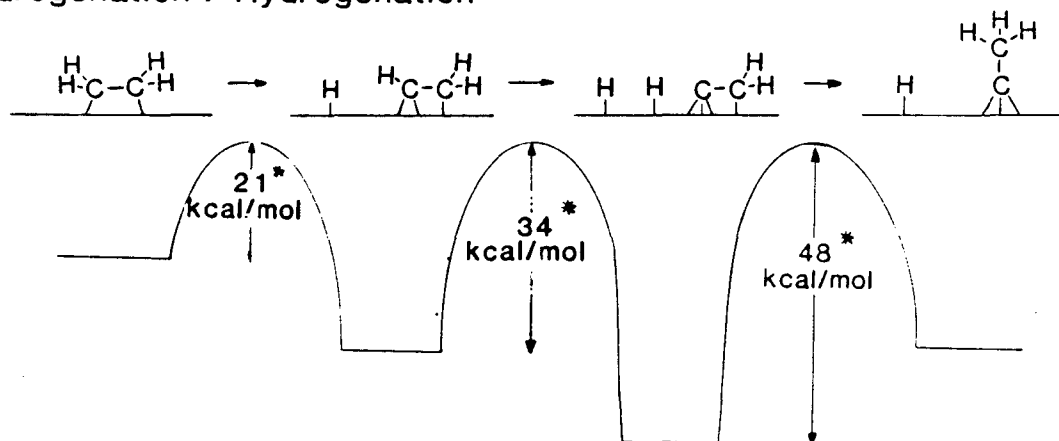


XBL 882-9560

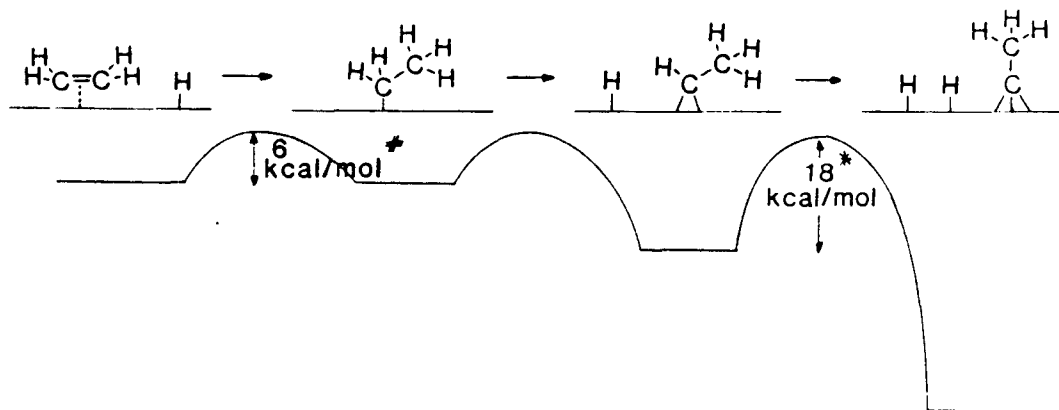
Fig. 17

Proposed Mechanisms For Ethylidyne Formation

Dehydrogenation / Hydrogenation

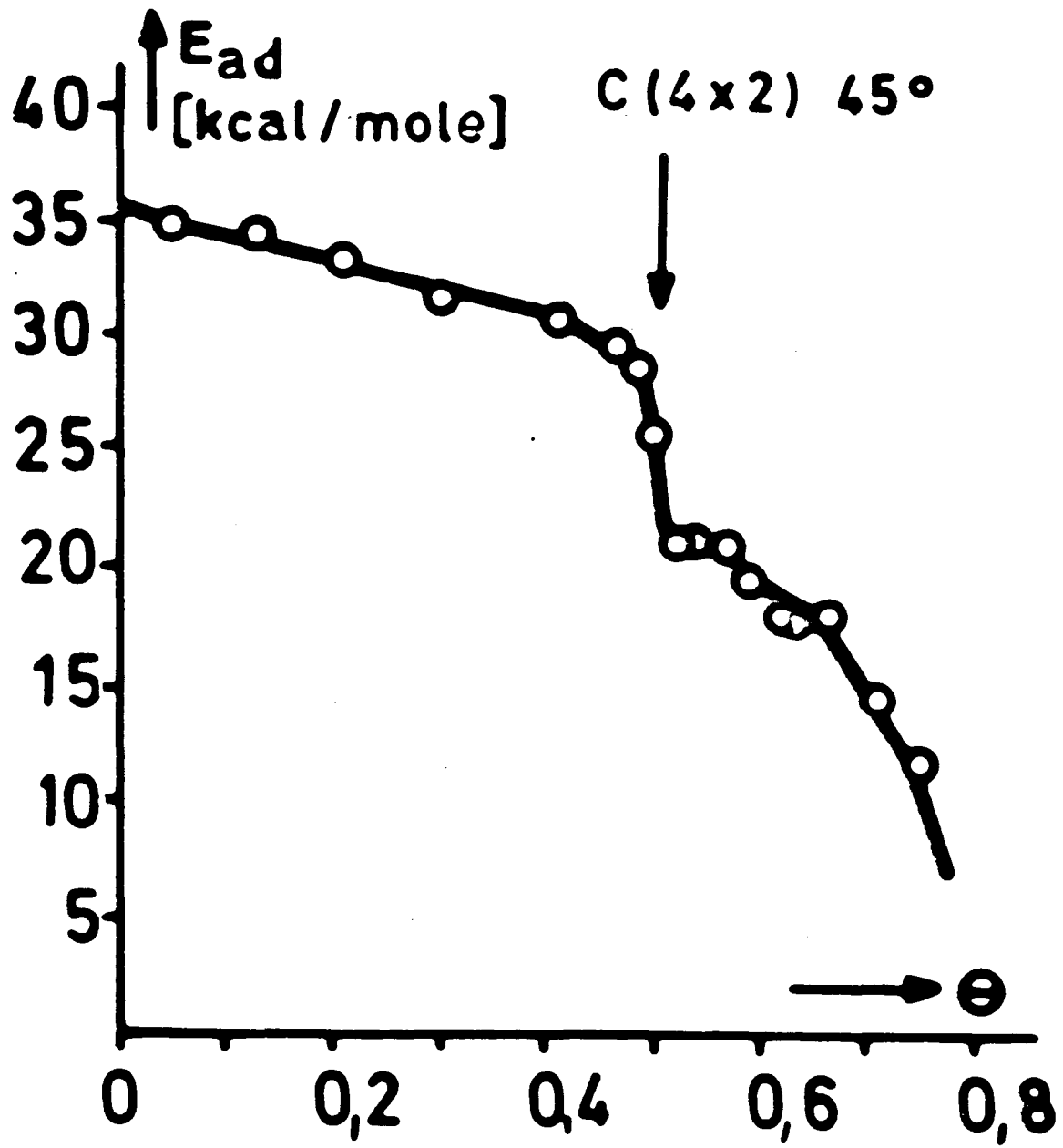


Hydrogenation / Dehydrogenation



XBL 8512-4943

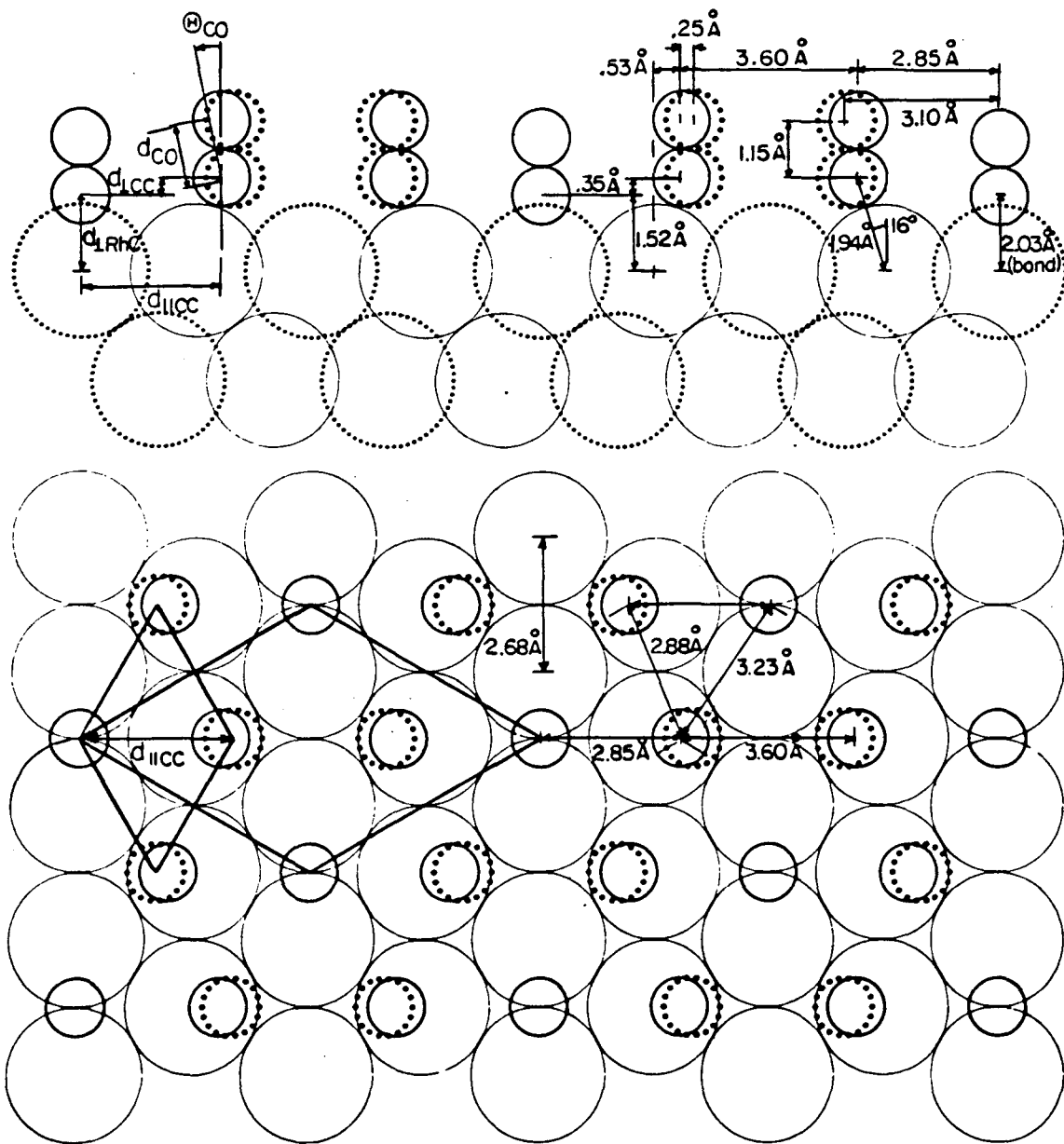
Fig. 18



XBL 7911-12823

Fig. 19

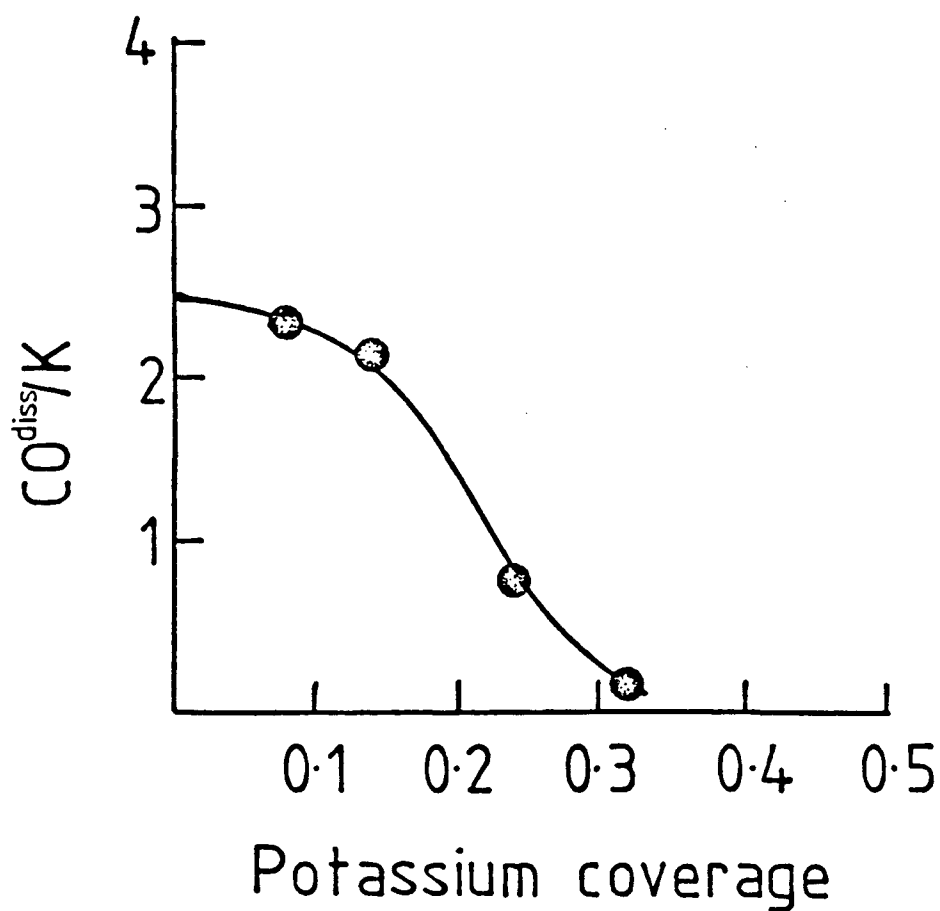
Rh(III) (2x2) - 3 CO



XBL 828-6270

Fig. 20

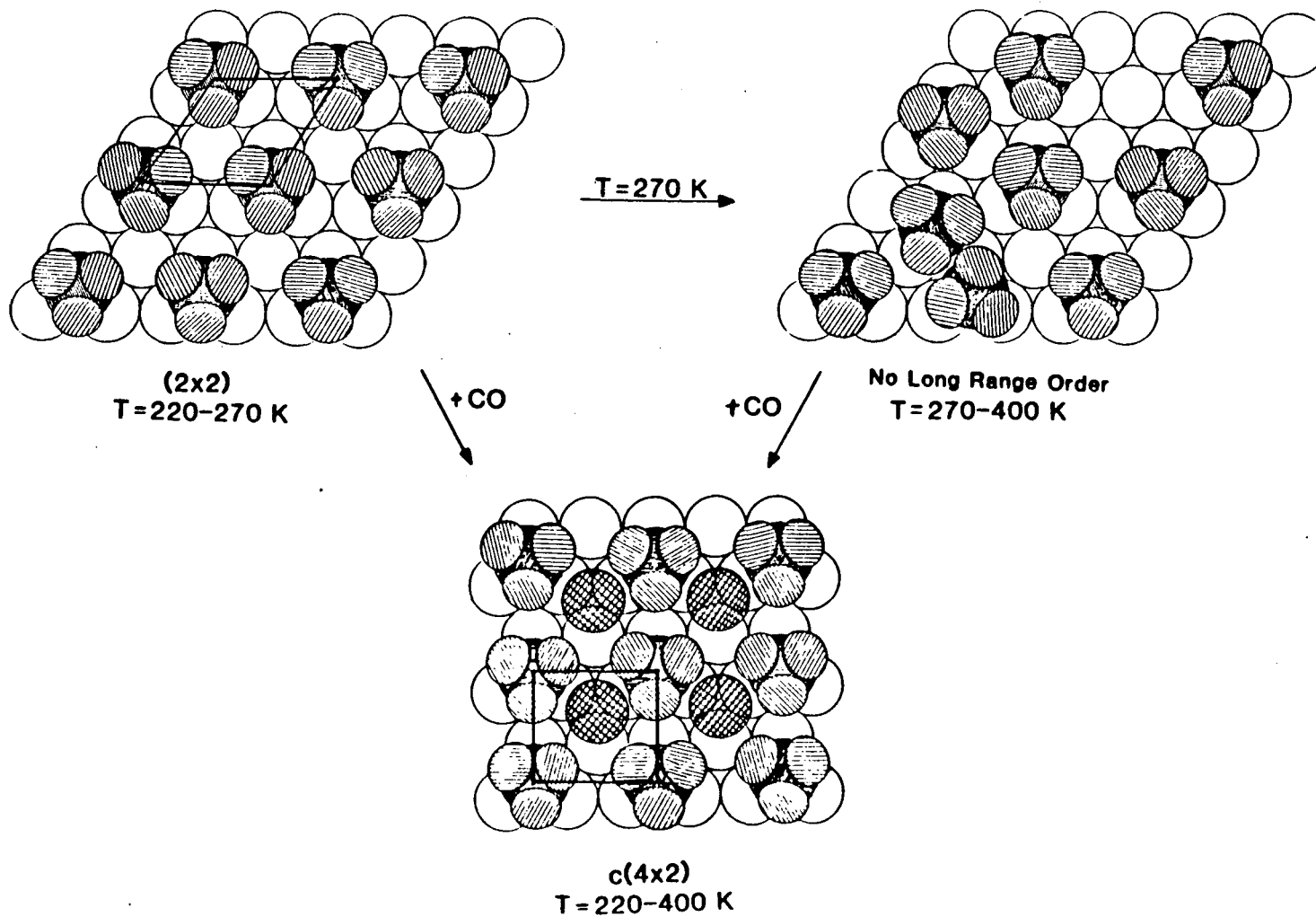
Plot of number of CO molecules that dissociate per potassium as a function of potassium coverage.



XBL 844-1415

Fig. 21

Rh(111) / Ethylidyne Ordering

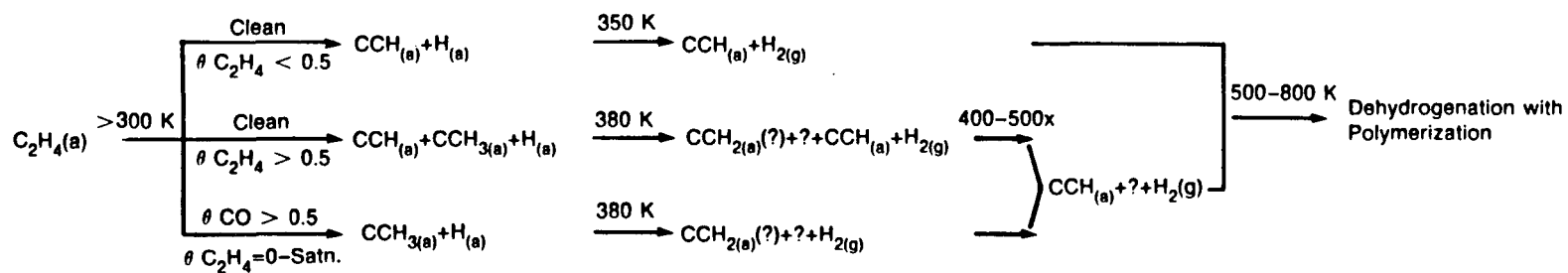


63

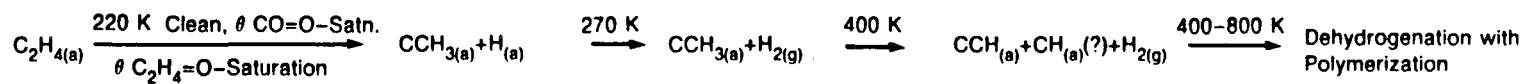
XBL 866-2421

Fig. 22

(A) Rh(100)



(B) Rh(111)



XBL 882-9563 A

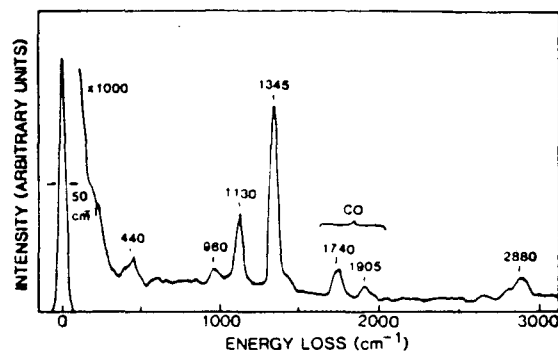
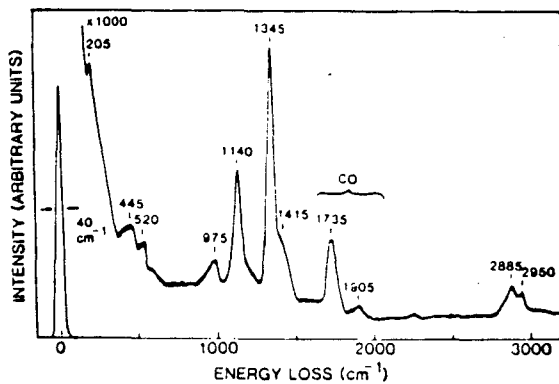
Fig. 23

Rh(111) Surface:

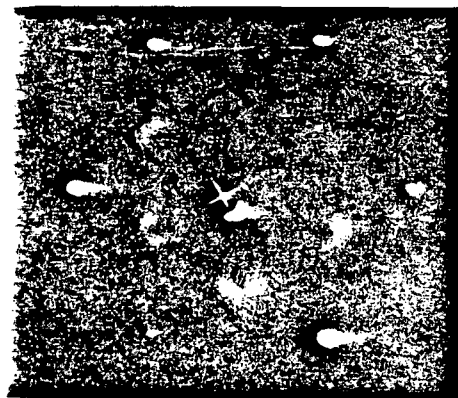
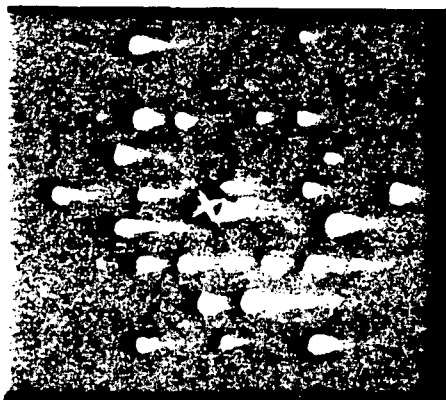
After C_2H_4 Hydrogenation

With a Monolayer of Ethylidyne

HREELS



LEED



TDS

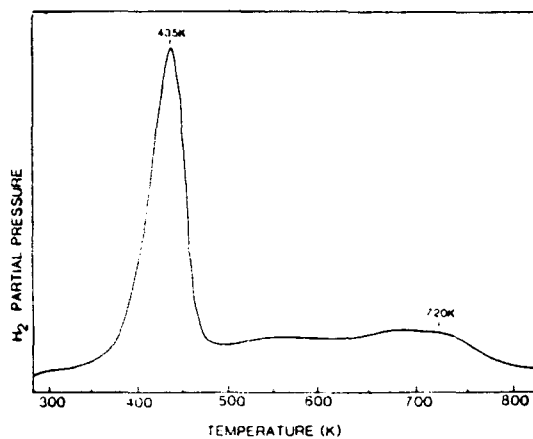
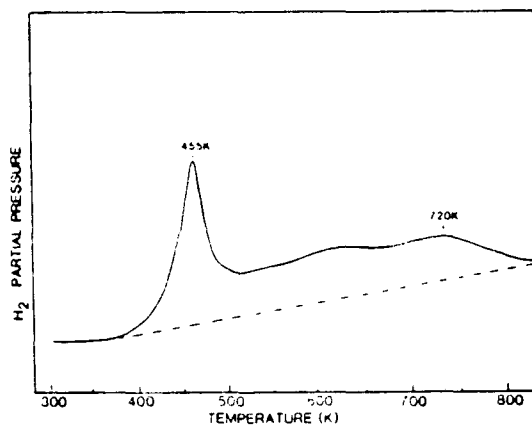
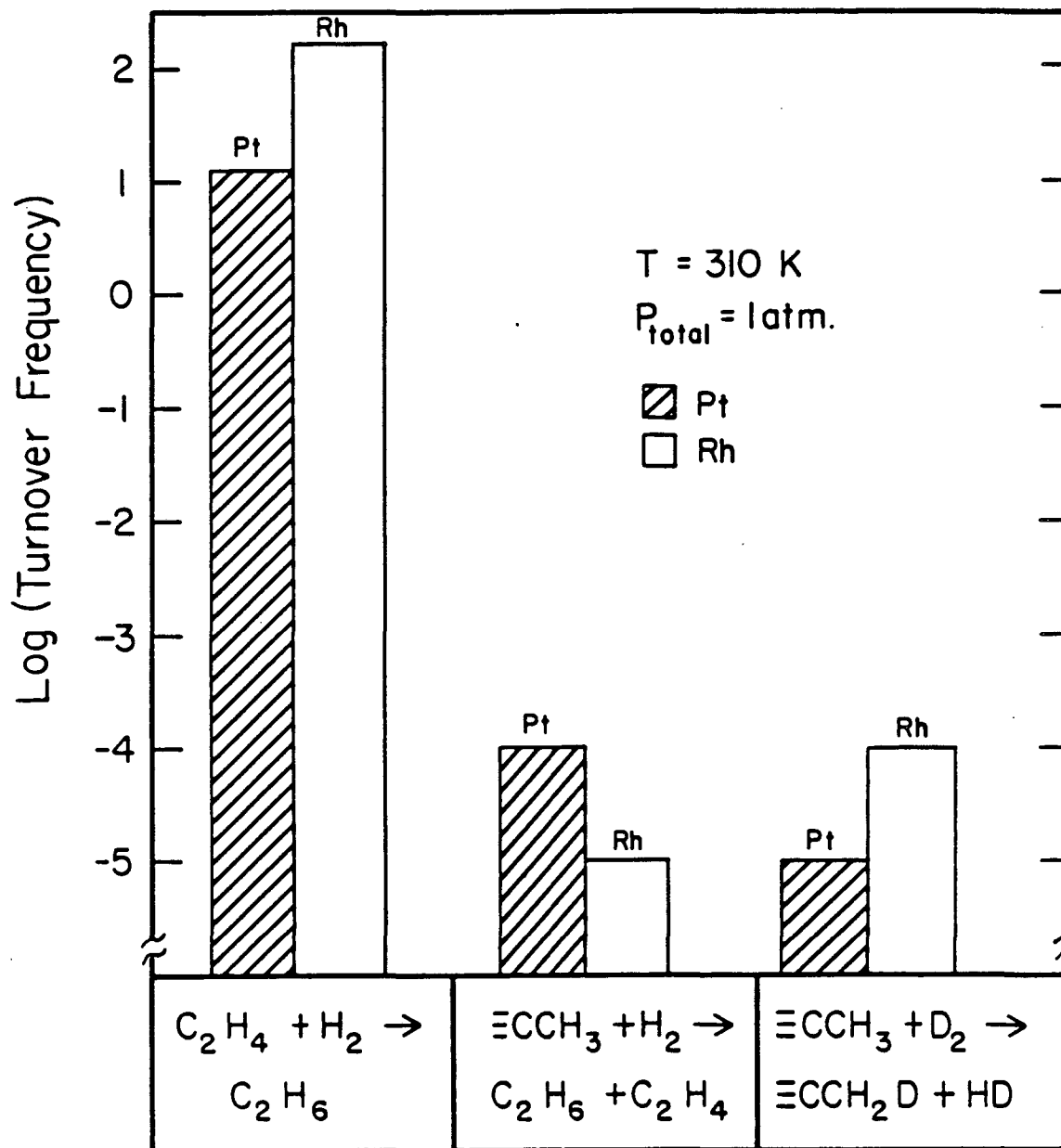


Fig. 24

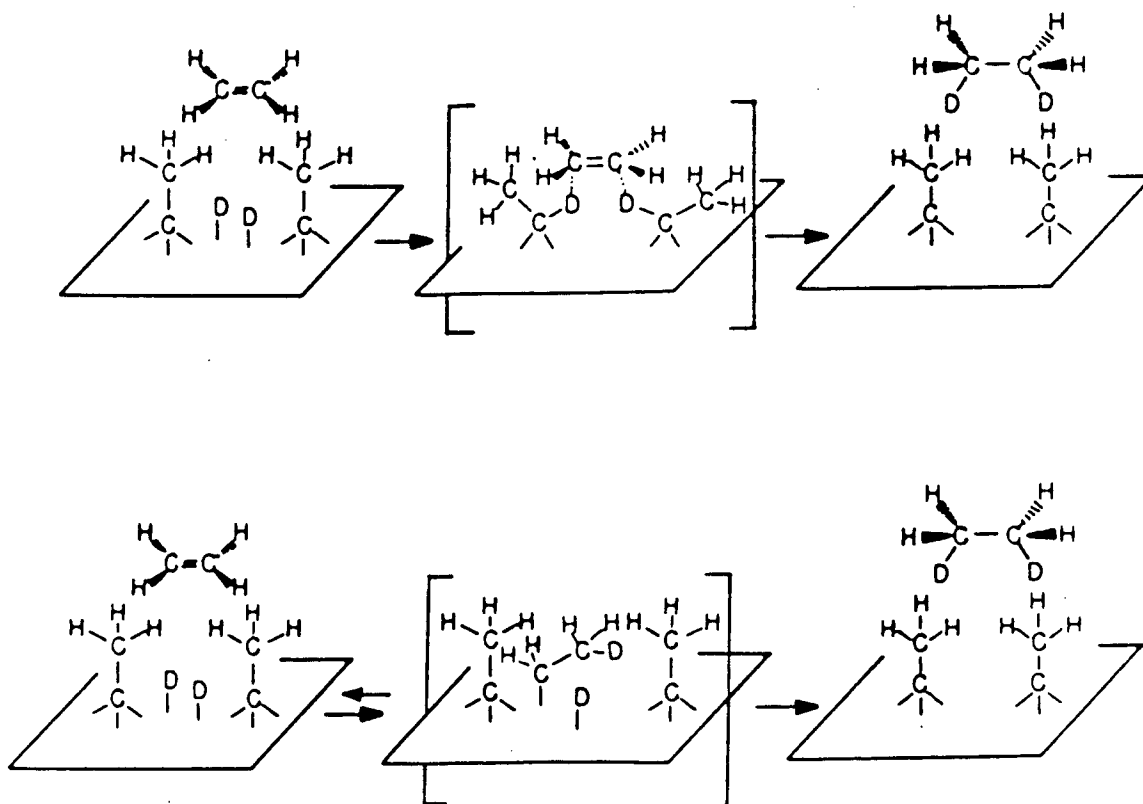
Comparison of Hydrogenation Rates
over Pt(III) and Rh(III) Single-Crystal Surfaces



XBL 846-2487

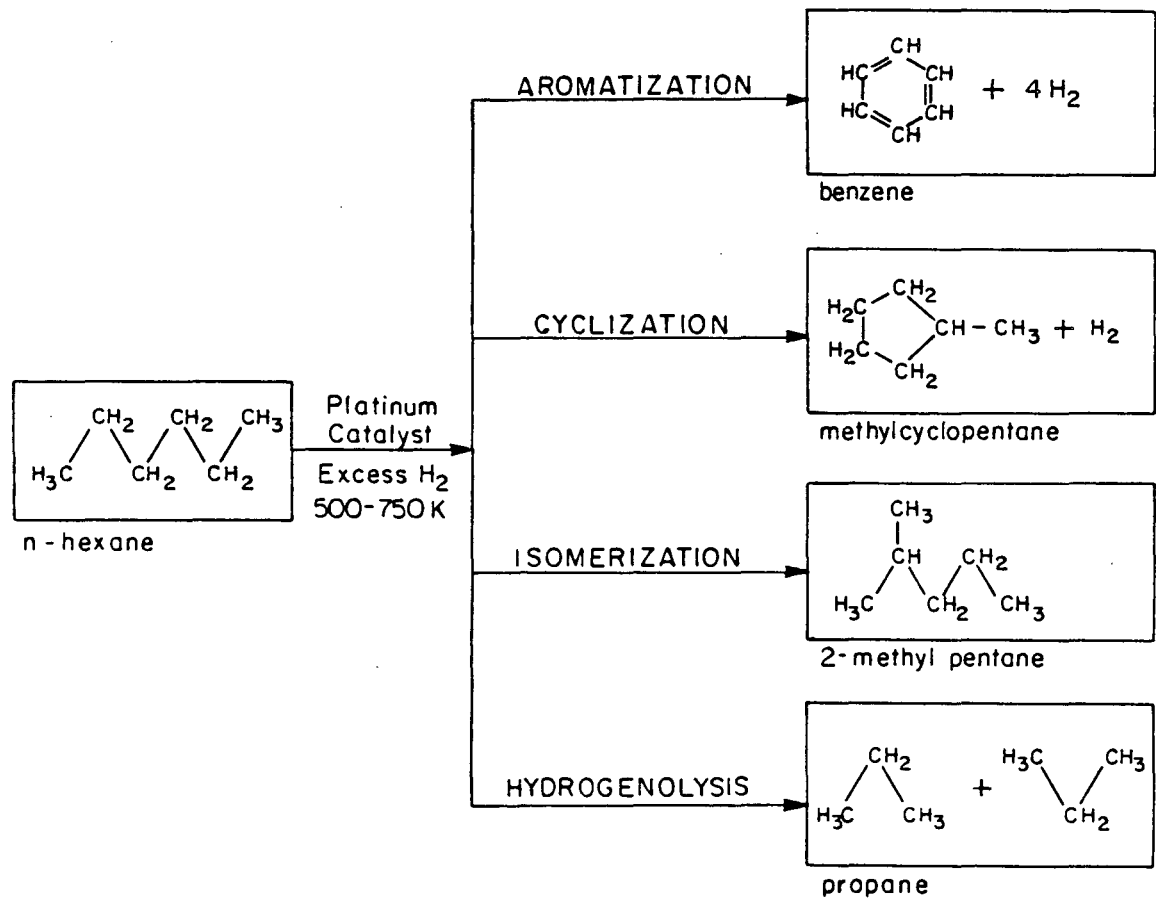
Fig. 25

Proposed Mechanisms for Ethylene Hydrogenation Over Platinum Metals



XBL 8610-4163

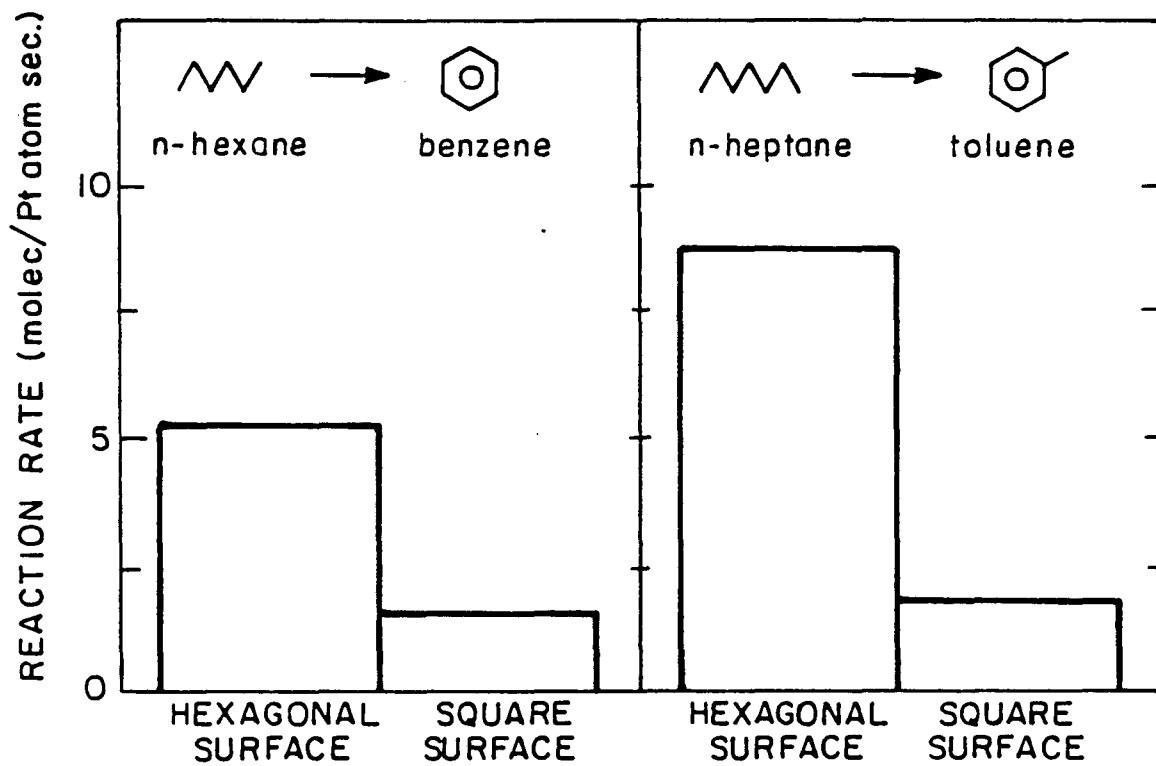
Fig. 26



XBL 822-5139

Fig. 27

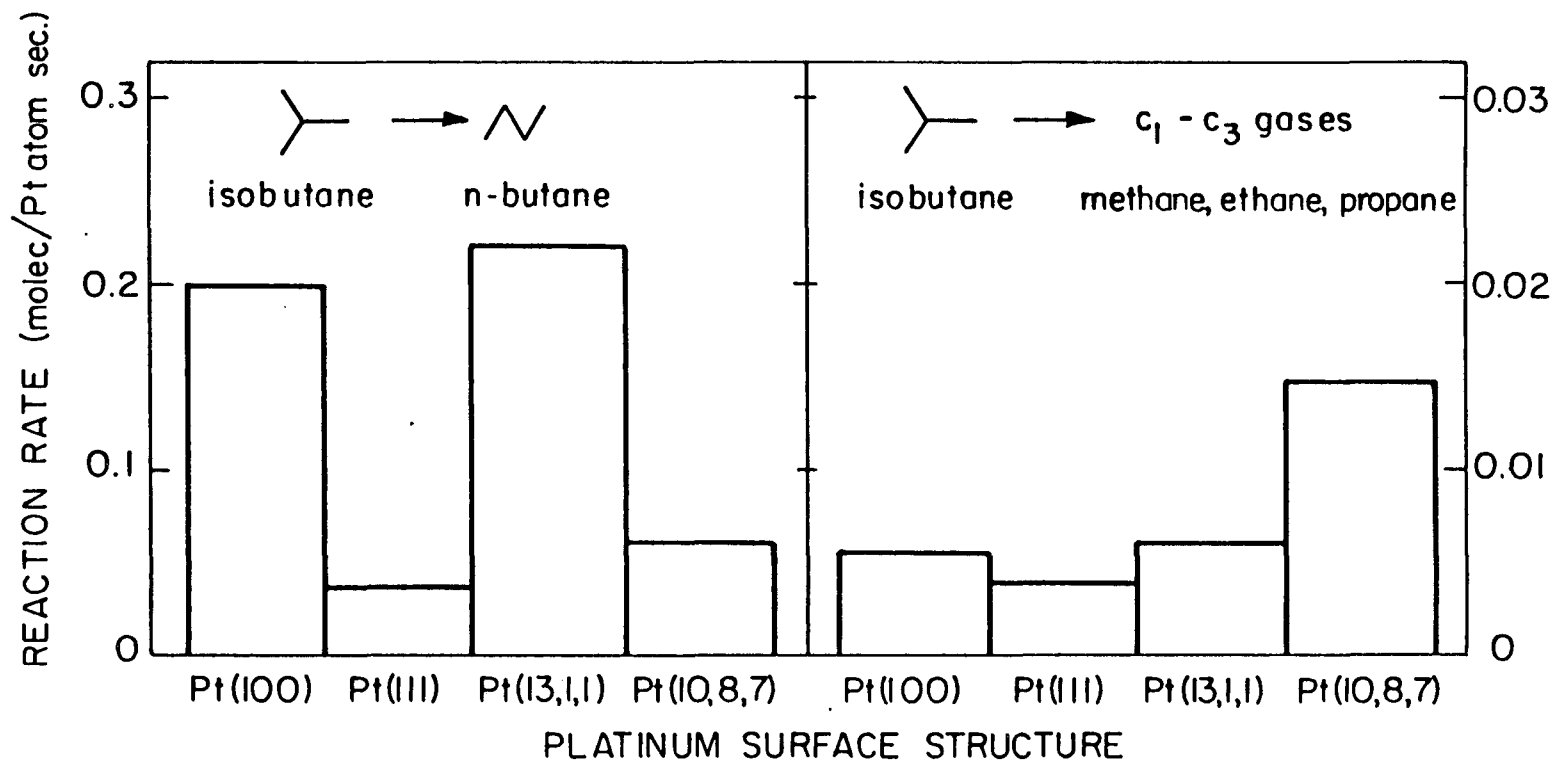
STRUCTURE SENSITIVITY OF ALKANE AROMATIZATION



XBL 822-5137

Fig. 28

STRUCTURE SENSITIVITY OF LIGHT ALKANE SKELETAL REARRANGEMENT



XBL 8 22 - 5 13 6

Fig. 29

*LAWRENCE BERKELEY LABORATORY
CENTER FOR ADVANCED MATERIALS
1 CYCLOTRON ROAD
BERKELEY, CALIFORNIA 94720*